

THE EFFECTS OF HIGH CHOLESTEROL/HIGH FAT DIET ON
ENDOPLASMIC RETICULUM STRESS AND NEURONAL DYSFUNCTION IN
THE HIPPOCAMPUS AND CEREBRAL CORTEX OF APOE^{-/-} MICE

A THESIS SUBMITTED TO
THE GRADUATE SCHOOL OF NATURAL AND APPLIED SCIENCES
OF
MIDDLE EAST TECHNICAL UNIVERSITY

BY

NAZ MENGİ

IN PARTIAL FULFILLMENT OF THE REQUIREMENTS
FOR
THE DEGREE OF MASTER OF SCIENCE
IN
MOLECULAR BIOLOGY AND GENETICS

JULY 2019

Approval of the thesis:

**THE EFFECTS OF HIGH CHOLESTEROL/HIGH FAT DIET ON
ENDOPLASMIC RETICULUM STRESS AND NEURONAL DYSFUNCTION
IN THE HIPPOCAMPUS AND CEREBRAL CORTEX OF APOE^{-/-} MICE**

submitted by **NAZ MENGI** in partial fulfillment of the requirements for the degree
of **Master of Science in Molecular Biology and Genetics Department, Middle East
Technical University** by,

Prof. Dr. Halil Kalıpçılar
Dean, Graduate School of **Natural and Applied Sciences** _____

Prof. Dr. Ayşe Gül Gözen
Head of Department, **Molecular Biology and Genetics** _____

Assoc. Prof. Dr. Tülin Yanık
Supervisor, **Molecular Biology and Genetics, METU** _____

Prof. Dr. Michelle Adams
Co-Supervisor, **Neuroscience and Psychology, Bilkent Uni.** _____

Examining Committee Members:

Prof. Dr. Sreeparna Banerjee, Assoc. Prof. Dr. Çağdaş Devrim
Son, Assoc. Prof. Dr. Soner Doğan, and Dr. Bige Güvenç Tuna
for their time and effort they invested in my thesis.
Department of Biological Sciences, METU _____

Assoc. Prof. Dr. Tülin Yanık
Molecular Biology and Genetics, METU _____

Assoc. Prof. Dr. Çağdaş Devrim Son
Department of Biological Sciences, METU _____

Assoc. Prof. Dr. Soner Doğan
Department of Medical Biology, Yeditepe University _____

Dr. Bilge Güvenç Tuna
Department of Biophysics, Yeditepe University _____

Date: 12.07.2019

I hereby declare that all information in this document has been obtained and presented in accordance with academic rules and ethical conduct. I also declare that, as required by these rules and conduct, I have fully cited and referenced all material and results that are not original to this work.

Name, Surname: Naz Mengi

Signature:

ABSTRACT

THE EFFECTS OF HIGH CHOLESTEROL/HIGH FAT DIET ON ENDOPLASMIC RETICULUM STRESS AND NEURONAL DYSFUNCTION IN THE HIPPOCAMPUS AND CEREBRAL CORTEX OF APOE^{-/-} MICE

Mengi, Naz

Master of Science, Molecular Biology and Genetics

Supervisor: Assoc. Prof. Dr. Tülin Yanık

Co-Supervisor: Prof. Dr. Michelle Adams

July 2019, 63 pages

Hyperlipidemia is an obesity-associated lipid metabolism disorder with high serum total cholesterol (TC) levels and is known to be a risk factor for neurodegenerative diseases. High-fat diet (HFD) induced elevated inflammation levels accompanied by increased levels of apoptosis markers and decreased levels of synaptic proteins in the hippocampus points out a possible neuronal loss. Protein kinase RNA-like endoplasmic reticulum kinase (PERK) pathway is activated by endoplasmic reticulum (ER) stress. The activation of PERK pathway results in reduced protein synthesis and increased expression of transcription factors involved in the apoptotic and inflammatory response. A possible impact of PERK pathway activation on neuronal failure has been questioned.

In this study, the impacts of high cholesterol/high-fat diet (HC/HFD) on the PERK pathway, inflammation, postsynaptic integrity, and neurogenesis were investigated in the hippocampus and the cerebral cortex of ApoE^{-/-} mice by performing Western blot analysis. In the hippocampus, no changes in the PERK pathway was detected, inflammation levels were decreased with Western diet. In the cerebral cortex, the levels of ER stress, inflammation, and postsynaptic integrity proteins were significantly increased in ApoE^{-/-} mice independently of the diet. Neurogenesis was

significantly higher in the hippocampus and the cerebral cortex of ApoE^{-/-} mice. Whereas there was no effect of HC/HFD on ER stress in the hippocampus, genotype effect activated the PERK pathway in the cerebral cortex.

Keywords: Obesity, Hyperlipidemia, Western Diet, ER Stress, Hippocampus

ÖZ

YÜKSEK KOLESTEROL/YÜKSEK YAĞ DIYETİNİN APOE^{-/-}FARELERİN HİPOKAMPÜS VE SEREBRAL KORTEKSİNDE ENDOPLAZMİK RETİKULUM STRESİNE VE NÖRONAL FONKSİYON BOZUKLUKLARINA ETKİSİ

Mengi, Naz
Yüksek Lisans, Moleküler Biyoloji ve Genetik
Tez Danışmanı: Doç. Dr. Tülin Yanık
Ortak Tez Danışmanı: Prof. Dr. Michelle Adams

Temmuz 2019, 63 sayfa

Hiperlipidemi, serum kolesterol seviyelerinin yüksek olması ile obeziteye bağlı lipid metabolizma bozukluğudur ve nörodejeneratif hastalıklar için risk faktörü oluşturduğu bilinmektedir. Yüksek yağlı diyetin inflamasyon ve apoptoz belirteçlerini artırması, sinaptik protein seviyelerini azaltması hipokampüste olası nöron kaybına işaret eder. Protein kinaz RNA benzeri endoplazmik retikulum kinaz (PERK) yolağı, endoplazmik retikulum (ER) stresi ile indüklenir. Bu yolağın aktivasyonu; protein sentezinin azalması, apoptoz ve inflamasyonda rol alan transkripsiyon faktörlerinin ekspresyonunun artmasıyla sonuçlanır. PERK yolağı aktivasyonunun nöronal yetmezlik üzerindeki olası etkisi sorgulanmıştır.

Bu çalışmada, yüksek kolesterol/yüksek yağ diyetinin (YK/YYD) PERK yolağı, inflamasyon, postsinaptik bütünlük ve nörogenez üzerindeki etkileri, ApoE^{-/-} farelerin hipokampus ve serebral kortekslerinde Western blot analizi yapılarak incelenmiştir. Hipokampüste PERK yolağında bir değişim saptanmazken, Western diyeti inflamasyonu azaltmıştır. Serebral kortekste ER stresi, inflamasyon ve postsinaptik bütünlüğünü gösteren proteinlerin seviyeleri ApoE^{-/-} farelerinde diyetten bağımsız olarak artmıştır. ApoE^{-/-} farelerinin hipokampus ve serebral kortekslerinde

nörogenez artmıştır. YC/YYD diyetinin hipokampüste PERK yolağı üzerine bir etkisi olmazken, serebral kortekste genotip PERK yolağını indüklemiştir.

Anahtar Kelimeler: Obezite, Hiperlipidemi, Yüksek Yağı Diyet, ER stress, Hipokampüs

To My Family,

ACKNOWLEDGEMENTS

I am deeply grateful to my supervisor Assoc. Prof. Dr. Tülin Yanık for her guidance, patience and advice throughout the study.

I would like to express my gratitude to my co-advisor Prof. Dr. Michelle Adams for the opportunity to be a part of her research group. I am grateful to all members of her lab, for their guidance and endless support.

I would like to thank the members of my thesis committee; Prof Dr. Sreeparna Banerjee, Assoc. Prof. Dr. Çağdaş Devrim Son, Assoc. Prof. Dr. Soner Doğan, and Dr. Bige Güvenç Tuna for their time and effort they invested in my thesis.

I would like to thank Assoc. Prof. Dr. Ebru Erbay for this project and her financial support from European Molecular Biology Organization (EMBO). I would like to express my gratitude to her lab members; Begüm Kocatürk, İnci Onat, Aslı Ekin Doğan, and Zehra Yıldırım for the maintenance of animals and their technical support.

I would like to express my heartfelt gratitude to my project partner, Bilge Aşkın. She was the perfect friend and colleague. I am very grateful for her patience, continued advice and her work. I would like to thank her help for the experiments. I was very lucky to have you as a lab partner, thank you for your endless support. You will always be loved and missed.

I cannot thank enough to my parents for their unconditional love and precious support. I would like to thank Kübra Çamur for being a perfect role model in academic life. I wish to thank Ekin Yavuz, my best friend. You are always there for me for the good times and the bad times. Finally, I would like to thank Barış Çamur. I am thankful for your unconditional love. I would not be the person that I am today without you.

This project 'YLT-108-2018-3732' was supported by METU-BAP.

TABLE OF CONTENTS

ABSTRACT	v
ÖZ	vii
ACKNOWLEDGEMENTS	x
TABLE OF CONTENTS	xi
LIST OF TABLES	xiv
LIST OF FIGURES	xv
LIST OF ABBREVIATIONS	xvii
CHAPTERS	
1. INTRODUCTION	1
1.1. Obesity.....	1
1.2. Hyperlipidemia	2
1.2.1. ApoE ^{-/-} Mice as Hyperlipidemic Animal Model	3
1.3. Neuroinflammation	4
1.4. High Fat Diet (HFD) Effects on Hippocampus	5
1.5. Neurogenesis	7
1.6. Endoplasmic Reticulum (ER) Stress	9
1.6.1. The Activation of PERK Pathway Upon High-Fat Content in Brain	10
1.7. PERK Pathway as a Potential Treatment Neurodegenerative Diseases	11
1.8. The aim of this study	12
2. MATERIALS AND METHODS.....	15
2.1. Animal Subjects	15
2.2. Dissections.....	17

2.3. Homogenization of Hippocampus and Cortex Tissues	18
2.4. Protein Isolation from Hippocampus and Cortex Tissues	19
2.5. Bradford Assay	19
2.6. Western Blot Analysis	20
3. RESULTS.....	25
3.1. The Effects of the Western Diet on the Hippocampus.....	25
3.1.1. ER Stress	25
3.1.1.1. p-PERK.....	25
3.1.1.2. p-eIF2 α	26
3.1.1.3. CHOP.....	26
3.1.2. Inflammation	27
3.1.3. Postsynaptic Integrity	28
3.1.4. Neurogenesis	29
3.2. The effects of Western Diet on the Cerebral Cortex	30
3.2.1. ER Stress	30
3.2.1.1. p-PERK.....	30
3.2.1.2. p-eIF2 α	31
3.2.1.3. CHOP.....	32
3.2.2. Inflammation	33
3.2.3. Postsynaptic Integrity	34
3.2.4. Neurogenesis	35
3.3. IHC Optimization.....	37
4. DISCUSSION	43
5. CONCLUSION AND FUTURE DIRECTIONS	47

REFERENCES.....	49
APPENDIX A	61
A. Supplementary for Western Blot Analysis	61

LIST OF TABLES

TABLES

Table 2.1. The experimental design including mouse strains and diets	15
Table A.1. The preparation of blank and standards.....	61
Table A.2. 10mL of 12% running gel.....	62
Table A.3. 5mL of 5% stacking gel.....	62
Table A.4. 10X SDS-PAGE Running buffer.....	62
Table A.5. 10X Transfer Buffer	63
Table A.6. 10X TBS adjusted at pH:7.6.....	63

LIST OF FIGURES

FIGURES

Figure 1.1. A coronal hippocampus section.....	6
Figure 1.2. The stages of adult neurogenesis in the hippocampus.....	8
Figure 2.1. The illustrations of experimental design.....	16
Figure 2.2. The isolated hippocampus.	18
Figure 2.3. OCT embedded brain tissue. A: Anterior, P: Posterior	18
Figure 2.4. The illustration of the transfer system.	21
Figure 3.1. The Western blot analysis of p-PERK in the hippocampus	25
Figure 3.2. The Western blot analysis of p-eIF2 α in the hippocampus.	26
Figure 3.3. The Western blot analysis of CHOP in the hippocampus	27
Figure 3.4. The Western blot analysis of IL-1 beta in the hippocampus	28
Figure 3.5. The Western blot analysis of PSD-95 in the hippocampus	29
Figure 3.6. The Western blot analysis of DCX in the hippocampus	30
Figure 3.7. The Western blot analysis of p-PERK in the cerebral cortex.....	31
Figure 3.8. The Western blot analysis of p-eIF2 α in the cerebral cortex)	32
Figure 3.9. The Western blot analysis of CHOP in the cerebral cortex.....	33
Figure 3.10. The Western blot analysis of IL-1 beta in the cerebral cortex.....	34
Figure 3.11. The Western blot analysis of PSD-95 in the cerebral cortex.....	35
Figure 3.12. The Western blot analysis of DCX in the cerebral cortex.....	36
Figure 3.13. The immunofluorescence staining of the hippocampus with 1:2000 NeuN.	37
Figure 3.14. The immunofluorescence staining of the hippocampus with 1:4000 NeuN.	38
Figure 3.15. The immunofluorescence staining of the hippocampus with 1:8000 NeuN.	39

Figure 3.16. The immunofluorescence staining of the hippocampus with NeuN in permeabilized sections	40
Figure 3.17. The immunofluorescence staining of the cerebral cortex and hypothalamus with IL-1 beta	41
Figure 3.18. The immunofluorescence staining of the cerebral cortex with Caspase-1	42
Figure 1.A. The standard curve of the absorbance levels of standards	61

LIST OF ABBREVIATIONS

- APOE: Apolipoprotein E
- ApoE^{-/-}: Mice lacking apoE
- ATF4: Activating transcription factor 4
- BBB: Blood-brain barrier
- BDNF: Brain-derived neurotrophic factors
- BSA: Bovine serum albumin
- CA: Cornu ammonis
- CHOL: Cholesterol
- CHOP: C/EBP homologous protein
- CM: Chylomicrons
- CNS: Central nervous system
- CVDs: Cardiovascular diseases
- DAPI: 4',6-diamidino-2-phenylindole
- DCX: Doublecortin
- DG: Dentate gyrus
- EC: Entorhinal area
- EIF2: Eukaryotic initiation factor 2
- EIF2B: Eukaryotic initiation factor 2B
- EIF2 α : Eukaryotic initiation factor 2 alpha
- ER: Endoplasmic reticulum
- FFA: Free fatty acids

GADD34: Growth arrest and deoxyribonucleic acids damage-inducible protein

GCL: Granular cell layer

GDP: Guanosine diphosphate

GEF: Guanine exchange factor

GTP: Guanosine triphosphate

HC/HFD: High cholesterol/high fat diet

HDL: High-density lipoprotein

HFD: High fat diet

IHC: Immunohistochemistry

IL-1 BETA: Interleukin 1 beta

IL-6: Interleukin 6

IP: Intraperitoneal

ISRIB: Integrated stress response inhibitor

LDL: Low-density lipoprotein

MAG: 2-monoacylglycerols

MYD88: myeloid differentiation factor 88

NEUN: Neuronal nuclei

NLRP3: Nucleotide-binding oligomerization domain leucine-rich repeat and pyrin domain-containing protein 3

OCT: Optimal cutting temperature compound

PBS: Phosphate-buffered saline

PERK: Protein kinase RNA-like endoplasmic reticulum kinase

P-EIF2 α : Phospho eukaryotic initiation factor 2 alpha

PIC: Preinitiation complex

PL: Phospholipids

P-PERK: Phospho protein kinase RNA-like endoplasmic reticulum kinase

PSD-95: Postsynaptic density-95

PVDF: Polyvinylidene fluoride

RIPA: Radioimmunoprecipitation assay

SDS-PAGE: Sodium dodecyl sulfate polyacrylamide gel electrophoresis

SEPHIN 1: Selective inhibitor of a holophosphatase

SGZ: Subgranular zone

SVZ: Subventricular zone

TAK1: Transforming growth factor beta-activated kinase-1

TBS: Tris buffered saline

TBS-T: Tris buffered saline-Tween 20

TC: Total cholesterol

TG: Triglycerides

TLR4: Toll like receptor 4

TNF- α : Tumor Necrosis Factor-alpha

TSSS: Tissue section staining solution

T-TBS: Tris buffered saline-Triton X

UPR: Unfolded protein response

VLDL: Very low-density

WHO: World Health Organization

CHAPTER 1

INTRODUCTION

1.1. Obesity

The general definition of obesity can be described as the accumulation of excessive fat in adipose tissue which may impair the individuals' health [1]. There are several factors that lead to excessive fat accumulation, however, one of the main reasons is excessive consumption of Western diets, which include high amounts of sugar and fat content, along with the decreased physical activity [2]. Nowadays, obesity is recognized as a worldwide health problem which also has affected Turkish population to a great extent. According to The Organization for Economic Co-operation and Development health statistics, 22.3% of the adult population is obese in Turkey [3]. Obesity is not a condition which is only about gaining weight but it is also linked to several disorders which can have numerous impacts on individuals' quality of life and even the cause of their deaths. Hyperlipidemia is a lipid metabolism disorder which is considered as one of the obesity comorbid conditions and recognized as a significant risk factor for developing atherosclerosis and cardiovascular diseases (CVDs) [4]. According to the World Health Organization (WHO), cardiovascular diseases are responsible for one of every four deaths around the world [5]. In Turkey, the statistical analyses that were performed by WHO showed that CVDs are the causes of 34% of all deaths in 2016 [6]. When we consider the number of individuals that are being affected by these conditions, it is crucial to understand the underlying molecular mechanisms behind the remarked deficits in order to develop therapies against these disorders.

1.2. Hyperlipidemia

Hyperlipidemia is a lipid metabolism disorder in which serum lipid levels are elevated as a result of the deficits in the transportation of fat molecules [4]. Lipids are organic compounds with their crucial functions for living organisms. Triglycerides (TG), phospholipids (PL), and cholesterol (CHOL) are the main nutritional components which are classified as lipids [7]. While TG are primarily utilized to produce energy, PL and CHOL are used for intracellular functions [8]. Since lipids are hydrophobic, they are transported as lipoproteins. Lipoproteins are spherical in structure and while their surfaces are mainly composed of PL, free CHOL, and proteins; their cores mainly consist of TG and CHOL esters [4]. The protein components of lipoproteins are named as apolipoproteins. Lipoproteins can be classified according to which apolipoproteins they carry. Apolipoproteins have significant roles for lipid transport, lipid metabolism and the integrity of lipoprotein structure [9]. There are four major types of lipoproteins; chylomicrons (CM), very low-density (VLDL), low-density lipoprotein (LDL) and high-density lipoprotein (HDL) [10].

Transporting lipids between where they are absorbed or synthesized and where they are stored or utilized is a highly regulated process. After ingesting a meal which includes fat, the lipolysis of TG to free fatty acids (FFA) and 2-monoacylglycerols (MAG) is initiated in the intestinal lumen which are received via the enterocytes with passive diffusion and active transport by these of transporters [11]. CHOL is also taken up by a special transporter of enterocytes [12]. In enterocytes, while FFA and MAG are coupled back to TG, CHOL forms cholesterol-esters [11]. Once PL, apolipoproteins (apo), TG and CHOL-esters are assembled, they are called CM [13]. CM are secreted to intestinal lymph and they enter blood circulation by thoracic duct [14]. The liver produces VLDL which are TG-rich lipoproteins. FFA are delivered by VLDL and CM to adipose tissue and skeletal muscle for energy production and storage [13]. The lipolysis of these TG-rich lipoproteins is necessary for releasing FFA to circulation and lipoprotein lipase is the main enzyme which is used for this purpose

[15]. During this process, CM form chylomicron remnants and VLDL form LDL which are eventually taken up by the liver [16]

The reverse cholesterol transport is achieved by HDL particles which are synthesized by the liver. They have an important role in taking CHOL from peripheral tissues and transport them back to the liver [17].

Any disturbances take place in this highly regulated lipid transport process can cause hyperlipidemia. Hyperlipidemia is characterized by increased levels of serum total cholesterol (TC), TG, low-density lipoprotein cholesterol and reduced levels of high-density lipoprotein cholesterol [18].

The increased levels of serum cholesterol are the consequence of hyperlipidemia and it poses a great risk factor for developing cardiovascular diseases, atherosclerosis, and stroke [19]. Studies have supported the idea that neurodegenerative diseases and central nervous system (CNS) injury can be caused by hyperlipidemia which shows the fact that hyperlipidemia can affect the CNS along with peripheral tissues [20]. The importance of lipid metabolism for CNS may be the result of high concentrations of lipids in this system. The important functions of lipids in neuronal integrity were demonstrated by several neurodegenerative disorders including Alzheimer's (AD), Parkinson's, and Huntington diseases involving in deregulated lipid metabolism [21]. Therefore, understanding how dysregulations in lipid metabolism affect CNS would promote novel approaches for developing therapies against seen deficits.

1.2.1. ApoE^{-/-} Mice as Hyperlipidemic Animal Model

There are different kinds of apolipoproteins with different crucial functions. One of them is apolipoprotein E (ApoE) that is a glycoprotein and has a role in the facilitation of lipid transport between where they are synthesized or absorbed and where they are utilized or stored [22]. ApoE functions as a ligand for lipoprotein receptors and mediates the uptake of CM, VLDL, and their remnants to LDL receptor. As a consequence, mice lacking ApoE (ApoE^{-/-}) demonstrate slow clearance of lipoprotein [23]. When ApoE^{-/-} mice fed with Western diet (0.21% cholesterol, 21% fat), they

develop hyperlipidemia, hypercholesterolemia and atherosclerotic plaques [24]. Therefore, ApoE^{-/-} mice have been extensively used as a practical mouse model for atherosclerosis and hyperlipidemia studies [25].

1.3. Neuroinflammation

Inflammation is an important defense mechanism against detrimental changes in the body. However, its neuropathological causes are well accepted [26]. The presence of low-grade inflammation in peripheral tissues in obese people is well known [27]. Recent studies suggested that it also can cause inflammation in the CNS [28].

The activation of Toll-like receptor 4 (TLR4) present on the immune cells can induce an inflammatory response and elevated serum FFA levels can induce TLR4 activation [29] that is followed by induction of downstream inflammatory signals by the help of cytoplasmic adaptor protein which is myeloid differentiation factor 88 (MyD88). The interaction of MyD88 and TLR4 activate two serine-threonine protein kinases which have a role in the phosphorylation of transforming growth factor beta-activated kinase-1 (TAK1). The induction of I κ B kinase complex by phosphorylated TAK1 leads to phosphorylation of I κ B which finally releases NF κ B. NF κ B is moved to the nucleus and starts to increase the transcription of proinflammatory cytokines which are Tumor Necrosis Factor-alpha (TNF- α), Interleukin 1 beta (IL-1beta), Interleukin 6 (IL-6) and additionally nucleotide-binding oligomerization domain leucine-rich repeat and pyrin domain-containing protein 3 (NLRP3) [30]. The oligomerization and activation of NLRP3 inflammasome cause the activation of caspase-1 which processes and releases IL-1beta. When the critical threshold level for caspase-1 activation is passed, the cell undergoes pyroptosis which is the term used for inflammation-induced cell death [31].

The question of how inflammation affects the different brain regions has aroused interest. One of the brain regions is hypothalamus which has naturally drawn attention since this area is home to the aggregation of neurons called arcuate nucleus which consists of the neurons of Neuropeptide Y/Agouti-related protein and Pro-opiomelanocortin/Cocaine- and amphetamine-regulated transcript have significant

roles in energy metabolism and the regulation of body weight [32]. Normally, the blood-brain barrier (BBB) is a specialized structure restricts the access of immune cells and their mediators into the brain [33]. However, some brain regions lack an effective BBB which makes them more prone to the negative effects of peripheral inflammation. The arcuate nucleus is one of these regions which lacks an effective BBB [34], therefore, how hypothalamus is affected by inflammation is a well-studied compared to the other brain regions [35], [36]. On the other hand, research indicated the fact that BBB can be altered by inflammation [37]. Peripheral inflammation increases the proinflammatory cytokines in plasma, this proinflammatory cytokines can also initiate an inflammatory response that induces the production of proinflammatory cytokines in the brain [38]. This results in neuroinflammation causing an increase in the permeability of other brain regions [39]. Therefore, recently the neuroinflammation and its impacts on the entire CNS including hippocampus has been sparked interest.

1.4. High Fat Diet (HFD) Effects on Hippocampus

Hippocampus is a brain structure and it is a part of the temporal lobe of the cerebral cortex [40]. It is easily distinguishable with it's a layer of neurons which are densely packed and created an S-shape structure. In literature, the hippocampus is divided into different regions morphologically as cornu ammonis (CA), dentate gyrus (DG), subiculum and entorhinal area (EC). The complete structure is called as hippocampal formation. The major regions of hippocampus are depicted in Figure 1.1 [41].

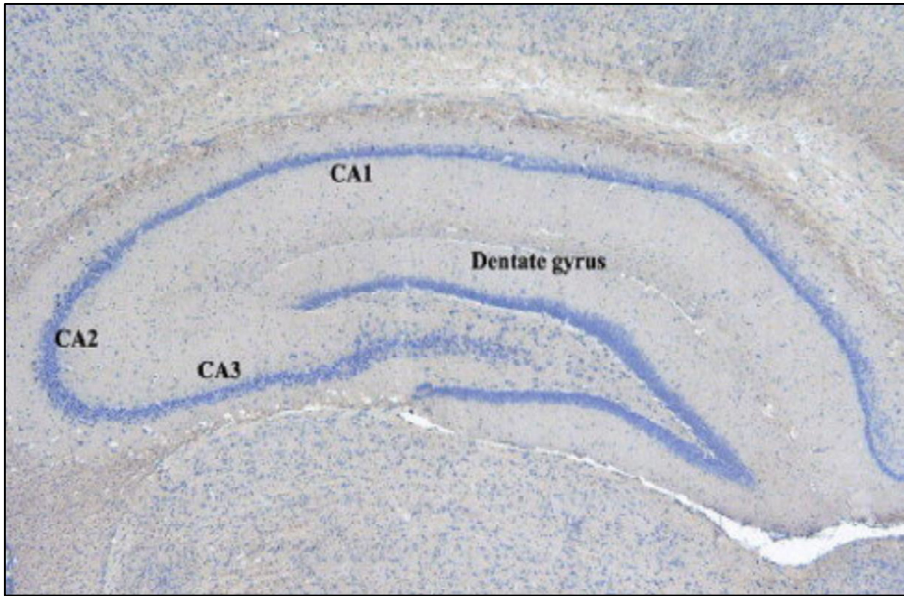


Figure 1.1. A coronal hippocampus section. Stained by Toluidine blue showing distinct regions of the hippocampal formation including Cornu Ammonis (CA) as CA1, CA2 and CA3 and dentate gyrus [41].

Although it has several roles, the hippocampus is best known for its irreplaceable function for learning, memory and spatial navigation. Learning and memory deficits for spatial relations have been considered as a major sign for hippocampal dysfunction [42].

Diets that have a high lipid content increase the serum lipid levels and found to cause alterations in different brain regions including the hippocampus [43]. The association between high lipid intake and regional brain atrophy of temporal lobe which is home to the hippocampus was documented [44]. Following studies revealed that elevated body fat is related to decreased neuronal viability in the grey and white matter of the brain including the temporal lobe [45]. There are also several human and animal studies which indicated how high cholesterol intake is a significant risk factor for impaired memory and cognitive deficits [46], [47], [48], [49], [50]. Although the findings relate high fat intake with cognitive and memory deficits, the underlying molecular mechanisms are not clearly understood.

Literature supported the idea that increased neuroinflammation upon high fat intake has harmful effects on neurons which eventually disrupt the neuronal integrity and lead to cellular death.

The relation of HFD to the elevation of expression of cytokines accompanied by increased levels of expression of NFkB in the hippocampus of rats [51]. Additionally, Dutheil, et. al (2016) showed HFD increased the TLR4 protein levels, expression of cytokines and apoptotic markers in this region [52]. The reduction of synaptic plasticity also has been recognized [53].

Also, the integrity of BBB has been investigated by analyzing the tight junction proteins of this structure. HFD declined tight junction protein levels pointing out a loosened BBB in the hippocampus [54]. Data has suggested that inflammation has an impact on increased permeability of BBB which makes the region much more prone to the effects of inflammation, hence give rise to synaptic failure and neuronal loss.

Few studies are also present on the effects of high cholesterol intake. Yang, et. al. (2017) showed that high cholesterol diet increased the FFA levels in the brain which is followed by elevation in the number of apoptotic neurons and inflammatory cytokines along with decreased BBB integrity. They hypothesized that induced secretion of these cytokines causes the destruction of the cerebral cortex [18].

1.5. Neurogenesis

Higher lipid intake has been associated with hippocampal-dependent cognitive and memory decline. Hence, how neuronal development is affected by elevated serum lipid levels received attention. Neurogenesis is a process in which new neurons are generated and formerly, it took place only in developmental stages but not in the adult brain. However, in 1962 Altman challenged this concept by showing that new neurons are present in different brain regions of rats including the hippocampus [55]. After the improvements in techniques for tracking cellular fate, evidence provided that the existence of adult neurogenesis [56]. The presence of neurogenesis in the subventricular zone (SVZ) and in the subgranular zone (SGZ) of the DG is well-

accepted today [57]. Through the rostral migratory system, the migration of neurons that are born in SVZ is provided [57], and then they join into olfactory bulb as interneurons. The neurons that are born in SGZ migrate to granular cell layer (GCL) and they integrate into GCL as granule cells [57].

Figure 1.2 shows the four main stages of adult neurogenesis which are composed of proliferation, differentiation, migration, and maturation. SGZ of DG is home to the neuronal stem cells and via this process, they become granular cells at GCL of DG [57].

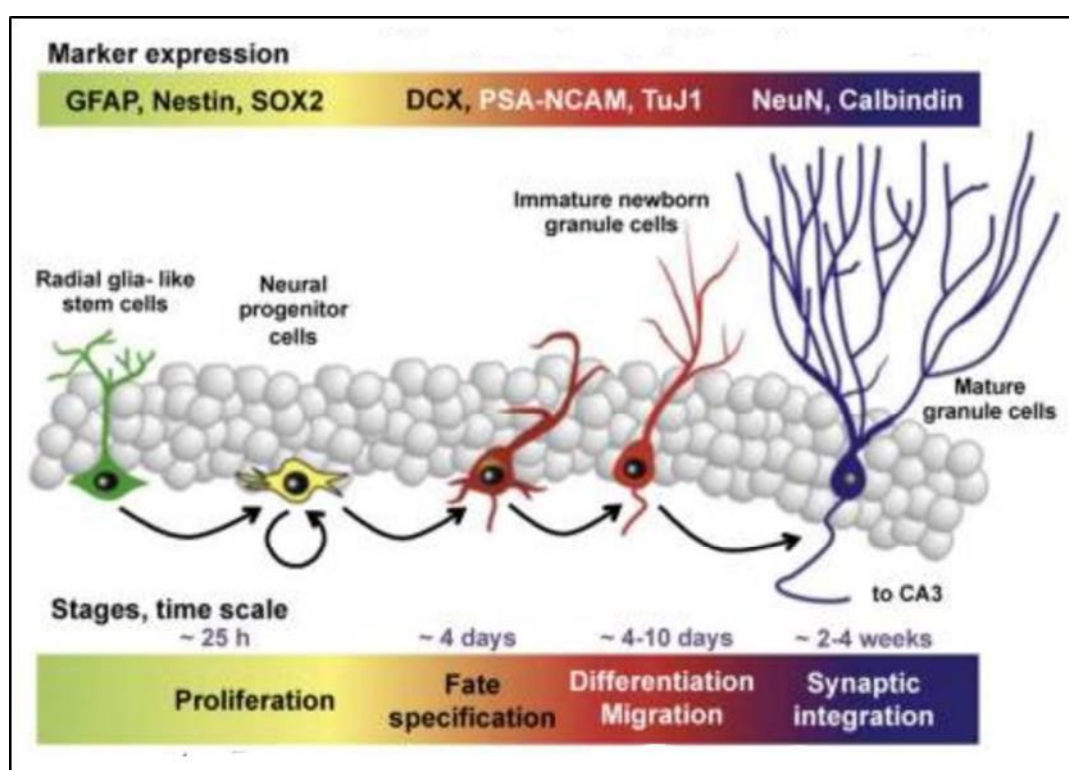


Figure 1.2. The stages of adult neurogenesis in the hippocampus. Associated markers of different stages are depicted. Radial glia-like cells give rise to neural progenitor cells. Some of them can give rise to immature neurons/neuroblasts which can differentiate into mature granule cells [57].

Many factors alter neurogenesis process and one of them is increased serum lipid levels. The elevated pro-cytokine levels were detected in hippocampus of animals fed

with the HFD and the decreased levels of neuronal stem cells was considered as a consequence of increased inflammation in the hippocampus. It has been proved that HFD was also linked to the diminished hippocampal neurogenesis due to the decreased levels of brain-derived neurotrophic factors (BDNF) which is a very crucial factor for neuronal survival and plasticity [58, 59].

1.6. Endoplasmic Reticulum (ER) Stress

ER is a cellular organelle that has several functions such as protein synthesis, maturation, folding and intracellular trafficking [60]. When these systems are disrupted under pathological conditions, ER stress is triggered [61]. Unfolded proteins start to accumulate in the cells during the ER stress which results in damaging the cells [62, 63], therefore, it is crucial for the cells to restore the ER homeostasis for their survival. There is a molecular system which is activated upon ER stress, namely called unfolded protein response (UPR) [64]. When ER fails to fulfill its protein folding capacity, UPR induces the three branches of pathways that aim the prevention of accumulation of unfolded proteins [65]. In order to achieve these objectives, these signal pathways attenuate the global protein synthesis to decrease the translation of newly produced proteins and activate the transcription of chaperone proteins to recover protein folding capacity [66].

There are three different pathways in the UPR [65]. One of the branches of UPR is the protein kinase RNA-like endoplasmic reticulum kinase (PERK) pathway. PERK is an ER transmembrane protein that has a cytosolic domain and a kinase domain [667]. The elevated levels of unfolded proteins are sensed by the cytosolic domain of PERK and this leads to the autophosphorylation of the kinase domain [67]. Phosphorylated PERK (p-PERK) phosphorylates eukaryotic Initiation Factor 2 alpha (eIF2 α) [64].

Eukaryotic Initiation Factor 2 (eIF2), which is comprised of eIF2 α , eIF2beta and eIF2gamma, can be found bound to guanosine diphosphate (GDP) or guanosine triphosphate (GTP) [68]. When eIF2 is bound to GTP, it associates with initiator methionine transfer ribonucleic acid which will enable the formation of the ternary

complex [69]. The transition of eIF2-GDP to eIF2-GTP is regulated by eukaryotic Initiation Factor 2B (eIF2B) which is a guanine exchange factor (GEF) [68]. The ternary complex is one of the members of the translation preinitiation complex (PIC) aside with a messenger ribonucleic acid and the small ribosomal subunit without the formation of this complex, translation cannot be performed [70].

If phosphorylation of eIF2 α (p-eIF2 α) occurs, it strengthens the affinity of eIF2 to eIF2B which potentially causes the reduction of its GEF activity [68]. That results in the prevention of the formation of the ternary complex which affects the production of PIC, consequently, these events lead to the attenuation of protein synthesis.

p-eIF2 α activates selective translation of activating transcription factor 4 (ATF4) [71]. ATF4 increases the transcription of a set of genes which include growth arrest and deoxyribonucleic acids damage-inducible protein (GADD34) and C/EBP homologous protein (CHOP) [71]. GADD34 has a function as dephosphorylation of p-eIF2 α and providing the inhibition of attenuation of global protein synthesis [72]. Prolonged ER stress results in high quantity production of CHOP which induces apoptosis and cytokine production [73].

1.6.1. The Activation of PERK Pathway Upon High-Fat Content in Brain

The presence of neuroinflammation followed by HFD has been indicated along with synaptic failure and apoptosis, yet, the molecular pathways which contribute these harmful results for cognitive health are still unknown.

Upon its activation, the PERK pathway results in global protein synthesis reduction increased inflammatory cytokines and apoptotic markers. The declined in global protein synthesis leads to synaptic failure since the proteins which are crucial for neuronal survival cannot be translated. Moreover, the presence of cytokines and apoptotic markers causes neuronal death. These observations are consistent with the cellular disturbances that were observed in the hippocampus of different animal models followed by high fat intake which make the PERK pathway a potential target to manipulate for therapeutic approaches for obesity-related neuroinflammation.

Lu, et. al (2010) demonstrated that the presence of ER stress in the hippocampus of wild type mice fed with high cholesterol diet, the elevated levels of NFkB and neuronal loss which has supported the concept of the ER stress may contribute to the harmful influences of high cholesterol intake in the hippocampus [74]. However, additional studies are necessary to reveal how the brain is altered in hyperlipidemia.

1.7. PERK Pathway as a Potential Treatment Neurodegenerative Diseases

Alzheimer's disease, Parkinson's disease, prion disease, and amyotrophic lateral sclerosis are known as neurodegenerative disorders share a common feature which is the aggregation of misfolded proteins and related cellular apoptosis [75]. The underlying mechanisms leading to neuronal loss in these disorders are still under investigation. There are many cellular pathways whose disturbances can contribute to pathological conditions resulting in neurodegeneration. Lastly, the idea of the activation of ER stress contribution on neurodegeneration has appeared to be one of the cellular mechanisms [76]. The concept of using the PERK pathway inhibitors to restore global protein synthesis against synaptic failure and neuronal loss has been started to be comprehended as a therapeutic approach [76]. There are different PERK pathway inhibitors that are able to block this pathway at different downstream levels. In this study, GSK2606414, integrated stress response inhibitor (ISRIB) and selective inhibitor of a holophosphatase (Sephin 1) were used.

GSK2606414 is a PERK pathway inhibitor prevents the phosphorylation of PERK occurred at the beginning of the PERK pathway [77]. GSK2606414 has the ability to block stress-induced autophosphorylation of PERK which prevents the phosphorylation of eIF2 α and decreases the ATF4 and CHOP protein levels [77]. It provided the restoration of protein synthesis and minimizes the neurodegeneration in prion-infected mice [78]. Nevertheless, although GSK2606414 has highly significant neuroprotective effects in the brain, it is linked to a certain extent of toxicity [79] that is associated with the pancreas that depends on diminished protein translation because of its excessive synthesis levels of secretory proteins [77]. ISRIB is an integrated stress

response inhibitor. This inhibitor does not prevent the phosphorylation of eIF2 α , however, it enhances the activity of eIF2B [80]. Therefore, ISRIB enables the formation of the ternary complex and decreases the inhibition of protein synthesis without showing pancreatic toxicity [81]. Interestingly, the enhancement of memory was additionally observed [81]. Sephin 1 targets GADD34 which is the protein phosphatase of p-eIF2 α and functions as prolonging the phosphorylation of eIF2 α after the stress is induced [82], [83]. In this way, it attenuates the expression of certain stress-related genes such as CHOP [84]. Some degree of translation recovery is required to produce CHOP. By targeting GADD34, Sephin 1 diminishes the translation recovery which causes reduced expression levels of CHOP. The neuroprotective effects of Sephin 1 are supported for different misfolding protein diseases in mice [85].

1.8. The aim of this study

The High cholesterol/high-fat diet (HC/HFD) elevates the serum FFA levels. Increased serum FFA activates TLR4 receptors which leads to the production of inflammatory cytokines and eventually end up with low-grade inflammation in peripheral tissues. Insufficient BBB structure in different brain regions makes these regions vulnerable to the outcomes of neuroinflammation which ultimately results in neuronal failure. BBB is also a dynamic structure and elevated inflammation increases its permeability. Therefore, other brain regions do not lack efficient BBB has been affected. It has been hypothesized that hippocampus can be one of the regions in which neuroinflammation has harmful impacts since studies showed HC/HFD causes hippocampal learning and memory deficits. Parallel to the cognitive deficits, studies indicated that HFD decreases the neuronal integrity and causes neuronal loss.

In recent years, it has been thought that the stimulation of the PERK branch of the ER stress response can contribute to neurodegenerative diseases and diet-induced neuronal alterations. As the consequences of induced PERK pathway are similar to

the outcomes of high fat intake, the idea that using PERK pathway inhibition as a therapeutic approach gained attention.

The aim of this study was to improve the understanding of molecular mechanisms on the alterations in neurons caused by HC/HFD. Therefore, it was investigated that the effects of Western diet including HC/HFD on the ER stress, inflammation, neurogenesis and postsynaptic integrity in the hippocampus and the cortex of ApoE^{-/-} transgenic mice.

CHAPTER 2

MATERIALS AND METHODS

2.1. Animal Subjects

Male C57BL/6 and ApoE^{tm1Unc} (ApoE^{-/-}) mice were purchased from Charles River, Wilmington, Massachusetts that were provided by Prof. Dr. Michelle Adams, Bilkent University and Assoc. Prof. Dr. Ebru Erbay, Bilkent University. They were maintained in a room with controlled temperature (20–22 °C) and humidity (45–50 %), and a 12 h light/dark cycle. All animal procedures were approved by the Bilkent University Animal Ethics Committee (2018/2).

The experimental design was depicted in Table 2.1. The number of animals used in this study was determined by taking into consideration obtaining statistically meaningful results [86]. Experiments were initiated, when mice were nine weeks old. Control and transgenic groups received either standard rodent chow diet (4.5% fat) or Western diet classified as HC/HFD (0.21% cholesterol, 21% butterfat, catalog: TD.88137 #E15721, Ssniff Spezialdiaten, Germany). The animals had *ad libitum* access to their diet and to also water. The duration of each diet was 16 weeks.

Table 2.1. The experimental design including mouse strains and diets.

Animal Groups and Diet Types	The number of Animals
C57BL/6, Chow Diet	n=7
C57BL/6, Western Diet	n=7
ApoE ^{-/-} , Chow Diet	n=7
ApoE ^{-/-} , Western Diet	n=7

For immunohistochemistry experiments, there were slight changes in animal groups and feeding process that were conducted with only male ApoE^{-/-} mice. Western diet (0.21% cholesterol, 21% butterfat) was started to be given *ad libitum* from the age of 8 weeks and it was continued to for 10 weeks. After that by daily intraperitoneal (IP)

injections, GSK2606414 (30 mg/kg) (Atomole) or DMSO (Sigma Aldrich), Sephin1 (5 mg/kg) or DMSO, ISRIB (1 mg/kg) (Cayman CHEM) or DMSO were given to the subjects in separate groups. As vehicles, while %12.5 (v/v) cremophor-saline was used for GSK2606414 and DMSO, %16 (v/v) cremophor-saline was used for Sephin 1 and DMSO, ISRIB and DMSO. The duration of injections was 6 weeks for GSK2606414, ISRIB, and their DMSO control groups; the injections were performed for 4 weeks for Sephin 1 and its DMSO control group. During this process, the Western diet was continued to be given to the subjects. The experimental design was illustrated in Figure 2.1.

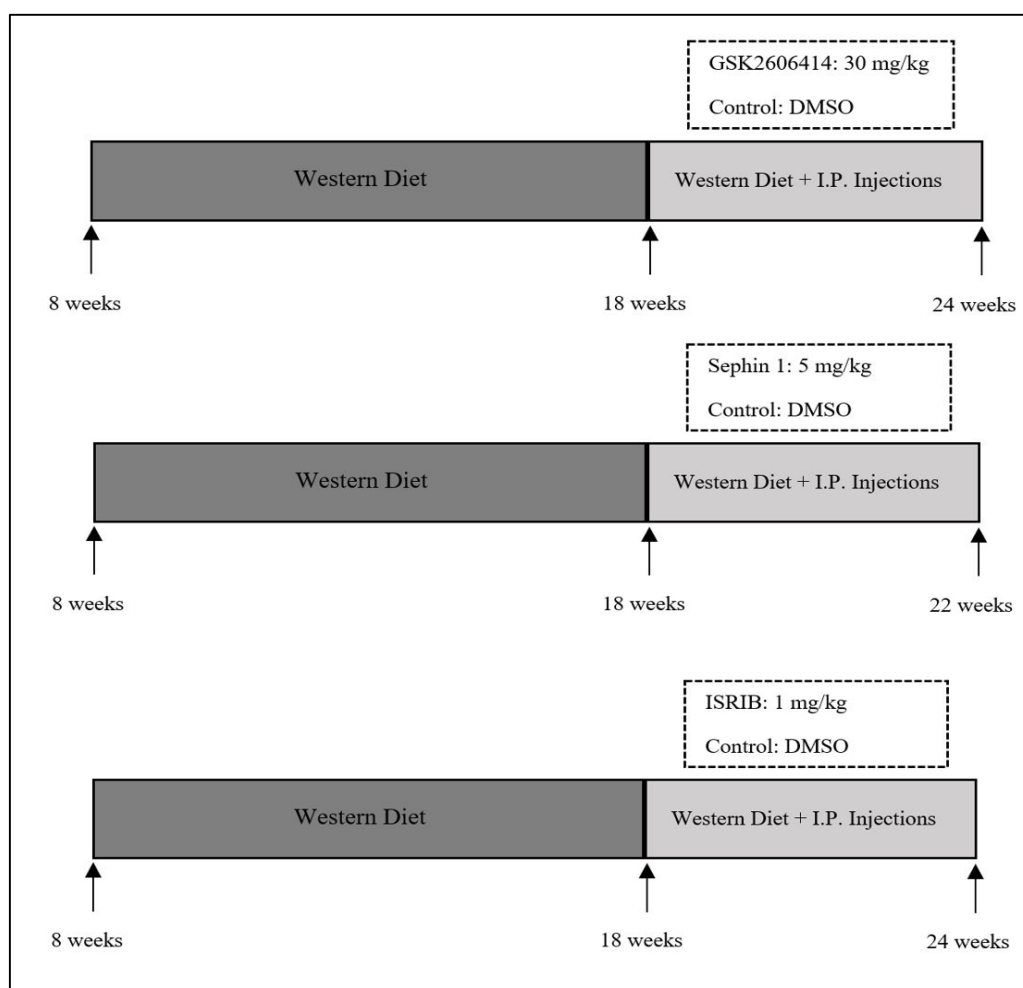


Figure 2.1. The illustrations of experimental design.

2.2. Dissections

The subjects fasted for 12 hours before sacrifice. The anesthesia of animals was provided with the injection of xylazine (10 mg/kg) and ketamine (100 mg/kg) intraperitoneally. The dilution of Ketaset (100 mg/mL) and Xylaject (20 mg/mL) was provided in Phosphate-Buffered Saline (PBS) solution. After intraperitoneal injection, the toes of the animals were pinched to monitor the anesthetic depth. With this process, the deep anesthesia can be assessed for 1-2 hours. Then the thoracic and abdominal cavity of the subjects was opened under the deep plane of anesthesia, approximately 1.0 mL of blood was collected from the apex of the heart to measure metabolic parameters. Next, 10-20 mL PBS was injected from the apex and then the right atrium was punctured to empty blood and PBS. If animals used for immunohistochemistry (IHC), 10-15 mL of 10% formalin was given to the subjects from the apex of their heart. If the subjects were used for Western blot analysis, this step was skipped.

Under the deep plane of surgical anesthesia, the cervical dislocation of the mice was followed by the decapitation of the animals. A petri dish, which included cold 0.1 M PBS, was located on ice. After extracted from the skull, the brain was placed on the Petri dish, the cerebellum and the olfactory bulb were removed with a scalpel blade. For protein immunoblot experiments, the brain was cut along the midline to separate two cerebral hemispheres. Each hemisphere was placed as their medial sides were facing up. The tissue that was covering the medial surface of hippocampus was removed by a sterile dissection spatula. Then, the dissection spatula was placed under the ventral part of hippocampus and the intact hippocampus was removed from the cortex. The hippocampi (Figure 2.2) collected from two hemispheres and the remaining brain tissue were placed separately into the 1.5 mL centrifuge tubes. By putting centrifuge tubes into liquid nitrogen, the samples were snap-frozen. After that, they stored at -80°C, until the experiments were started.



Figure 2.2. The isolated hippocampus.

For immunohistochemistry studies, the base of plastic cryomolds was filled with optimal cutting temperature (OCT) compound. Then brains were embedded into cryomolds and their anterior and posterior sides were labeled on molds. Next, brains were covered with OCT (Figure 2.3.) and any air bubbles were removed by a sterile syringe tip. After 5 minutes, tissue blocks were snap-frozen by locating them into isobutanol which was placed in dry ice. They stored at -80°C until the experiments were started.



Figure 2.3. OCT embedded brain tissue. A: Anterior, P: Posterior

2.3. Homogenization of Hippocampus and Cortex Tissues

The tissues were put into 1.5 mL Eppendorf tubes. For cortex samples 800 μL and for hippocampus samples 350 μL homogenization buffer [1mM EDTA, 10mM Hepes,

250mM Sucrose, and Protein Inhibitor Cocktail, pH 7.4] was added to the tubes. In order to perform mechanical homogenization, first glass homogenizer was used for cortex samples, next the hippocampus and cortex tissues were passed through a 1 mL syringe for 7-8 times on the ice.

2.4. Protein Isolation from Hippocampus and Cortex Tissues

First, homogenization buffer was removed from the tissues by centrifugation at 8000 X g for 6 minutes at 4 °C. The supernatant was removed and pellets from cortex samples were suspended in 1000 µL radioimmunoprecipitation assay (RIPA) buffer [50 mM Tris-HCl, pH 7.4, containing 150 mM NaCl, 0.25% (w/v) sodium deoxycholate, 1% NP-40, 1.0 mM EDTA and Protein Inhibitor Cocktail] and pellets from hippocampus samples were suspended in 400 µL RIPA buffer. Next, the ultrasonication process was performed for 6 times with 1-second intervals. Samples were incubated on ice for 30 minutes and every 10 minutes they were mixed. Following the incubation period, samples were centrifuged at 13000 rpm for 20 minutes at 4 °C. The supernatant was taken and aliquoted. After the determination of protein concentrations, they were stored at -80 °C.

2.5. Bradford Assay

The concentration of proteins was measured by Bradford Assay (Sigma, St. Louis, MO, USA) using a 96-well plate according to manufacturer instructions. Bovine serum albumin (BSA, A7906, Sigma-Aldrich, St. Louis, MO, USA) was used as a standard solution and ddH₂O was used as a blank solution. The amounts of BSA and ddH₂O that were loaded on the plate for blanks and standards are represented in Table A.1. Unknown protein samples were prepared by adding 0.5 µL protein from each sample and 4.5 µL ddH₂O. Standards, blanks, and unknown protein samples were loaded into 96-well plate as duplicates and 250 µL of Bradford Reagent (B6916, Sigma, St. Louis, MO, USA) was added to each well. Then, the 96-well plate was placed on the plate shaker. They were mixed at 240 rpm for 45 seconds. Next, the plate was removed from the plate shaker and incubated at room temperature for 10

minutes without shaking. If any air bubbles had been detected, they were removed by using a sterile syringe tip. The values of absorbance were measured at 595 nm by multi-plate reader (SpectraMax M5, Molecular Devices, Sunnyvale, CA, USA). During the reading process, blanks were marked in the template and their absorbance values were omitted from the absorbance values of each well. The absorbance levels of standards and their concentration values were plotted and a standard curve (Figure A.1) was generated by applying a linear curve fit to the plot. This standard curve was used for the determination of unknown protein samples.

2.6. Western Blot Analysis

First, proteins were separated using Sodium Dodecyl Sulfate Polyacrylamide Gel Electrophoresis (SDS-PAGE). For this, 12% resolving gels were prepared (Table A.2). In order to prevent air bubble formation and to create a smooth surface, the surface of gels was covered with isopropanol. When polymerization was completed, isopropanol was removed from the gels and 5% stacking gel (Table A.3) was poured on the resolving gel. The comb was placed with an angle to prevent the trapping bubbles. After polymerization of stacking gel, gels were placed into the running modules in the gel box which was filled with 1X SDS-PAGE running buffer (Table A.4, 10X of SDS-PAGE running buffer) Then, the combs were removed while they were covered with the running buffer to prevent the damaging of the gels.

So as to determine the protein levels of p-PERK, p-eIF2 α , CHOP, and IL1-beta, 40 μ g of proteins and for doublecortin (DCX) and postsynaptic density-95 (PSD-95) levels, 30 μ g of protein samples were used. The samples were run in cohorts and cohorts were run at least two times at the different side of each gel to make more accurate comparisons between groups and determine that the place of the samples in gels would not have affected the results.

The samples were mixed with the appropriate volume of 2X loading buffer before loading them into the wells of the gel. They were incubated in a heater for 5 minutes at 95°C. After a quick spinning down samples were loaded onto the gels along with a

protein ladder (26619, Thermo Scientific Paisley, UK) and run for 30 minutes at 80 volts, then as soon as they left the stacking gel and entered to the resolving gel, the multitude of the volt was increased to 100 volts for approximately 120 minutes using the Mini-PROTEAN Tetra Cell system (BioRad, CA, USA).

Next, the protein samples were transferred to polyvinylidene fluoride (PVDF) membrane using the Mini Trans-blot Electrophoretic Transfer Cell module (BioRad, CA, USA). For transferring process, first 1X transfer buffer was prepared (Table A.5, 10X concentration of transfer buffer). Whatman papers, sponges and gel holder cassettes were put into 1X buffer. PVDF membranes were put into 100% Methanol (MeOH) for 3 minutes, after that they were put into ice-cold 1X transfer buffer. All components were placed in an order (Figure 2.4). The transfer of proteins to the membranes was performed at 100 volts for 90 minutes in ice-cold 1X transfer buffer. In order to determine any increase in resistance which may be caused by increased heat, milliamperes multitudes were checked regularly to eliminate it.

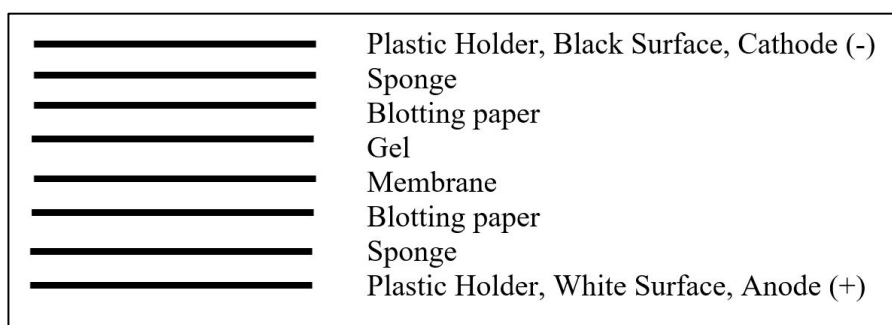


Figure 2.4. The illustration of the transfer system.

After the transfer process, the gels were checked for any remaining of marker to test the quality of the transfer. Then, the membranes were blocked at room temperature for one hour in their appropriate blocking buffer. Blocking buffers were chosen according to the optimization experiments. DCX, PSD-95, and Tubulin were blocked in Tris Buffered Saline-Tween 20 (TBS-T) including 5% Milk and p-PERK, p-eIF2 α , CHOP, and IL-1beta were blocked in TBST-including 5% BSA (10X TBS buffer, Table A.6).

The primary antibodies that were used in this study were the followings: anti-CHOP (Cell Signaling Technologies, cat#5554, 1:500), anti-DCX (abcam, cat#ab18723, 1:500), anti-IL1beta (abcam, cat# 9722, 1:500), anti-p-eIF2 α (Gene Tex, cat#GTX24837, 1:2000), anti-PSD-95 (abcam, cat#18528, 1:10000), anti-p-PERK (Cell Signaling Technologies, cat#3179, 1:500) and anti-Tubulin (Cell Signaling Technologies, cat#2146, 1:5000). Anti-DCX, anti-PSD-95, and anti-Tubulin were diluted in TBS-T-5% Milk and anti-CHOP, anti-IL1beta, anti-p-eIF2 α , anti-P-PERK were diluted in TBS-T-5% BSA. After the blocking process, membranes were soaked into TBS-T. Membranes were incubated with the primary antibodies overnight at 4°C.

In the following day, primary antibodies were collected from membranes. Membranes were washed with 1X TBS-T thrice for 10 minutes on a shaker. After the washing process, membranes were incubated in secondary antibodies (Cell Signaling Technologies, #7074, 1:10000) for 1 hour at room temperature on the shaker. Then secondary antibodies were collected and membranes washed in 1X TBS-T thrice for 10 minutes.

Chemiluminescent signals were obtained from horseradish peroxidase-conjugated secondary antibodies by using (Biorad, #1705061, USA). There were two different solutions in the kit which are luminol/enhancer solution and peroxide solution. These solutions were mixed (1:1) and put onto the membranes. Membranes were incubated for 5 minutes in dark. Those solutions were mixed in the proportion of 1:1 and immediately put onto the membranes. Membranes were incubated in a dark chamber for 5 minutes and then visualized. For detection of chemiluminescent signals, a ChemiDoc™ XRS+ imaging system was used (Biorad, CA, USA) with the ImageLab software (Biorad, CA, USA).

The images of the blots were taken by using Image Lab program and they were quantified with Image J software (NIH, Bethesda, MD, USA). First, the rectangular shape was selected as a selection and all lanes were quantified with the same sized rectangular selection and the intensity measurements were performed. In this study,

two normalization methods were performed; one of them was within-gel normalization that the normalization of each band to the average intensity of all bands in the same blot to prevent the exposure differences between blots because each sample was run at least two times [87]. The second was standard normalization, the intensity of protein interest was divided by the intensity of the housekeeping protein (Tubulin).

2.7 Statistical Analysis

The normal distribution and variance homogeneity were tested with the Kolmogorov-Smirnov test which met the expectations of the assumptions of the normality. A two-way analysis of variance (ANOVA) was utilized with the variables of diet with two levels (Chow Diet and Western Diet) and genotype with two levels (C57BL/6 and ApoE^{-/-}) on the protein levels of ER stress markers (p-PERK, p-eIF2 α , CHOP), inflammation marker (IL-1 beta), postsynaptic integrity marker (PSD-95), and neurogenesis marker (DCX). Post-hoc analysis was carried out with Bonferroni correction. *p<0.05 accepted as the significance level.

2.8 Immunohistochemistry (IHC)

OCT-embedded brain tissue blocks were coronally sectioned using a cryostat (Leica CM 1850 UV, Germany) as 10 μ m sections and they were put on ice for 30 minutes. For antigen retrieval process, the vegetable steamer was set up and preheated with the sodium citrate buffer [10 mM citrate, pH 6.0, containing 0.05% Tween20]. Sections were placed into the preheated antigen retrieval buffer and incubated in the steamer for 30 minutes. Then sections were cooled down at the room temperature. Next, sections were located into a glass jar filled with TBS plus 0.025% TritonX-100 (T-TBS) and washed for 5 minutes twice with gentle agitation. Blocking step was performed with 5% BSA in T-TBS for 1 hour at room temperature. Next, they were incubated with a primary antibody. The used primary antibodies were anti-Neuronal Nuclei (NeuN) (abcam, cat#104225, 1:2000, 1:4000, 1:8000) and anti-IL-1 beta (abcam, cat#9722, 1:150) which were diluted in 5% BSA in T-TBS overnight at 4 °C.

The next day, slides were washed in T-TBS thrice for 10 minutes with gentle agitation. Following washing steps, a proper fluorophore-conjugated secondary antibody (Cell Signaling Technologies, cat#4413, 1:1000) was applied to the sections for 1 hour at room temperature in dark. Next, they washed with TBS for 15 minutes thrice with gentle agitation in dark. They were mounted with fluoroshield mounting medium with 4',6-diamidino-2-phenylindole (DAPI) (abcam, cat#ab104139) and covered with a coverslip. Finally, images were captured with a Zeiss fluorescent microscope (Axio Zoom.V16, Zeiss, Oberkochen, Germany, UNAM, Bilkent University).

Additionally, to capture higher quality images, permeabilization was performed for NeuN staining that the IHC protocol was followed identically with an extra step after antigen retrieval process, sections were permeabilized with permeabilization buffer (TBS with 0.5% TritonX-100) for 5 minutes at room temperature.

2.9 Caspase-1 Activity

The activity of active caspase-1 was detected by using FAM-FLICA™ Caspase-1 Assay Kit (ImmunoChemistry Technologies, #97, LLC. Bloomington, MN, USA). 10 µm brain sections were put on ice for 30 minutes and the antigen retrieval process performed with sodium citrate buffer [10 mM citrate, pH 6.0, containing 0.05% Tween20] for 30 minutes by using a vegetable streamer. Then, with gentle agitation, slides were washed twice for 5 minutes with 0.025% T-TBS. After washing steps, the sections were blocked with 3% BSA in T-TBS for 1 hour at room temperature. The tissue section staining solution (TSSS) was prepared by diluting 150X FLICA stock in 0.025% TBS-TritonX (1:300, 1:150). Sections were incubated with TSSS for 2 hours in dark at room temperature. Then, the slides washed with 1X TBS thrice for 15 minutes and they were mounted with DAPI. Finally, images were taken with a Zeiss fluorescent microscope.

CHAPTER 3

RESULTS

3.1. The Effects of the Western Diet on the Hippocampus

To analyze the PERK pathway of ER stress on the subjects, p-PERK, p-eIF2 α , CHOP were used as markers.

3.1.1. ER Stress

3.1.1.1. p-PERK

There was no significant effect of diet and genotype on p-PERK levels in the hippocampus (Figure 3.1).

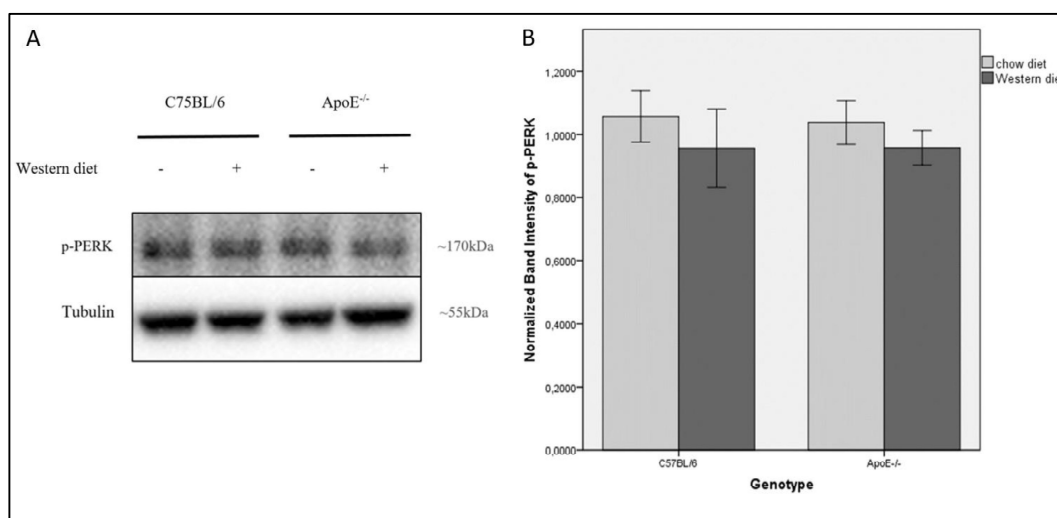


Figure 3.1. The Western blot analysis of p-PERK in the hippocampus [88]. (A) Representative immunoblot and (B) the quantification of the immunoblots (n=7, biological replicates) (n=2, technical replicates). Each bar represents Mean \pm SEM. Dark grey showed Western diet fed animals and light grey showed chow diet fed animals.

3.1.1.2. p-eIF2 α

Results showed that the expression of p-eIF2 α in the hippocampus was not significantly altered by diet and by genotype (Figure 3.2).

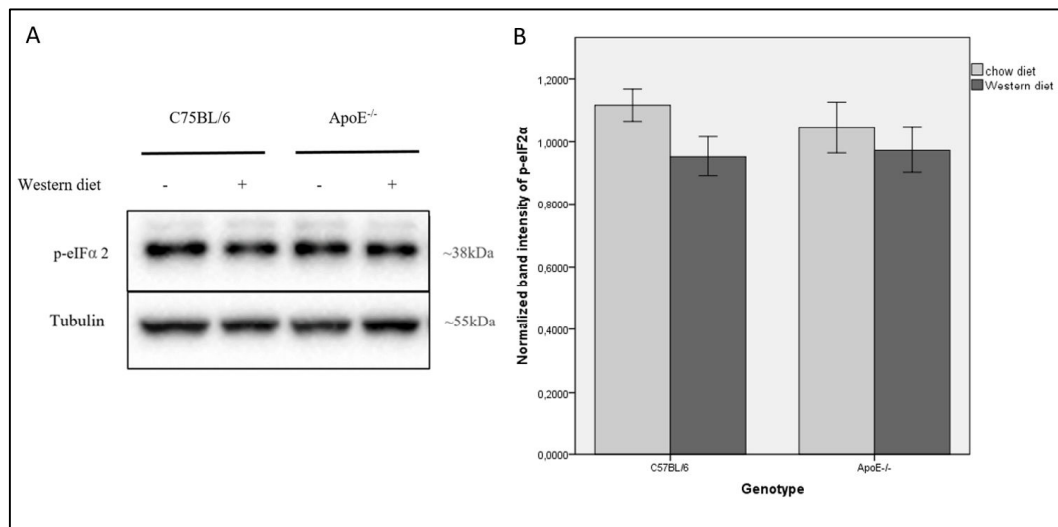


Figure 3.2. The Western blot analysis of p-eIF2 α in the hippocampus. (A) Representative immunoblot and (B) the quantification of the immunoblots (n=7, biological replicates) (n=3, technical replicates). Each bar represents Mean \pm SEM. Dark grey showed Western diet fed animals and light grey showed chow diet fed animals.

3.1.1.3. CHOP

The data analysis indicated that the main effect of both diet (** p <0.001) and genotype (p <0.05) on CHOP expression level was significant. Further post-hoc analysis showed that CHOP level was significantly decreased in both C57BL/6 (** p <0.001) and ApoE^{-/-} (p <0.05) mice with Western diet in comparison with chow diet (Figure 3.3). In addition to these results, CHOP expression level was significantly lower in chow diet for ApoE^{-/-} mice than C57BL/6 mice (p <0.05) (Figure 3.3).

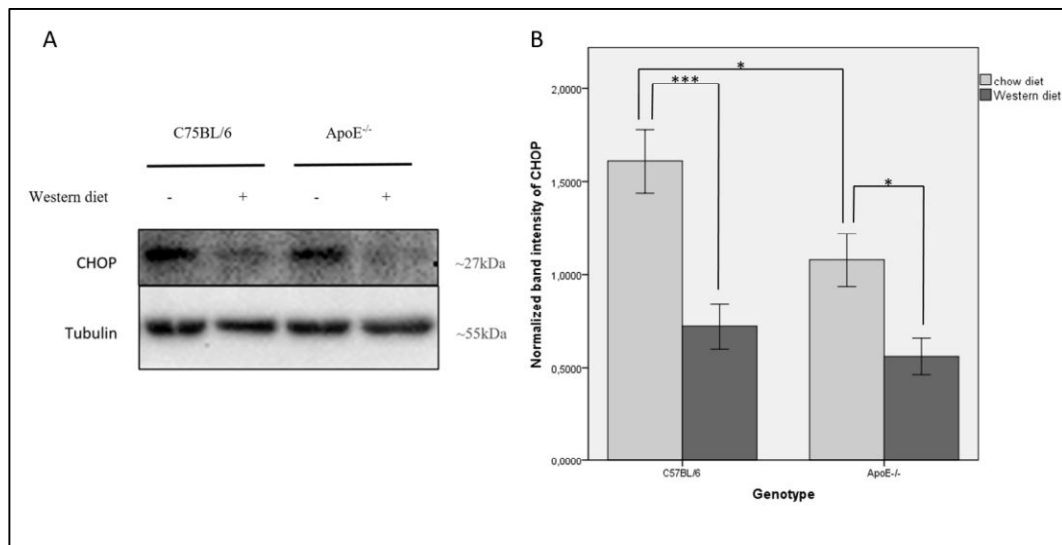


Figure 3.3. The Western blot analysis of CHOP in the hippocampus [88]. (A) Representative immunoblot and (B) the quantification of the immunoblots (n=7, biological replicates) (n=2, technical replicates). Each bar represents Mean ± SEM. Dark grey showed Western diet fed animals and light grey showed chow diet fed animals. (* $p<0.05$), *** $p<0.001$)

3.1.2. Inflammation

As inflammation marker, IL-1 beta was used. It is a cytokine with its several functions and involved in immune and proinflammatory responses, and it is one of the main caspase-1 targets [89]. The main effect of diet (** $p<0.001$) and genotype ($p<0.05$) on IL-1 beta expression were significant. Further interaction analysis revealed that IL-1 beta level was significantly decreased with Western diet both in the hippocampus of ApoE^{-/-} mice ($p<0.05$) and hippocampus of C57BL/6 mice (** $p<0.01$) (Figure 3.4). Additionally, while there is a significant decrease of IL-1 beta expression in ApoE^{-/-} strain compared to C57BL/6 strain with chow diet ($p<0.05$) (Figure 3.4), there was no significant change of our protein interest among C57BL/6 and ApoE^{-/-} mice with the Western diet.

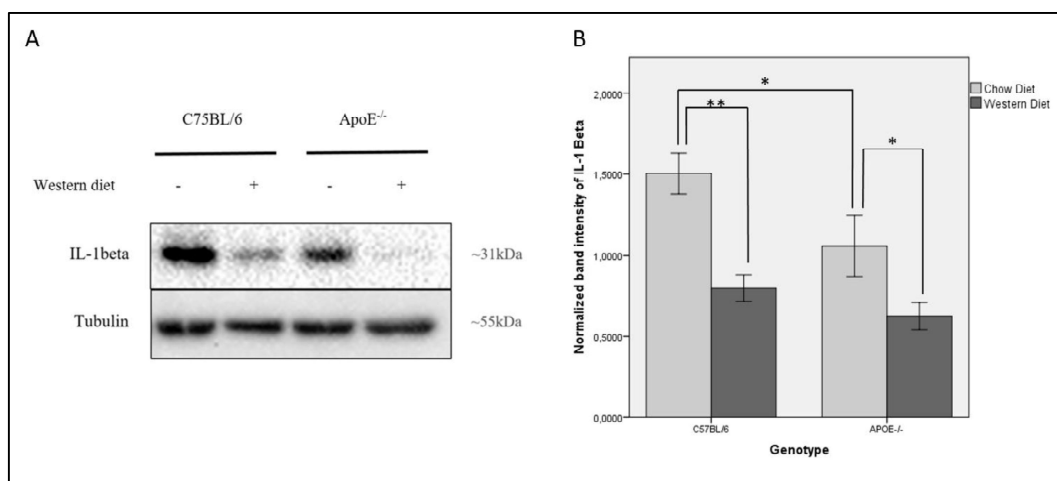


Figure 3.4. The Western blot analysis of IL-1 beta in the hippocampus [88]. (A) Representative immunoblot and (B) the quantification of the immunoblots (n=7, biological replicates) (n=2, technical replicates). Each bar represents Mean ± SEM. Dark grey showed Western diet fed animals and light grey showed chow diet fed animals. (* $p < 0.05$, ** $p < 0.01$)

3.1.3. Postsynaptic Integrity

To detect the postsynaptic density, PSD-95 was used as a marker which is one of the proteins present at the postsynaptic regions of excitatory synapses. Our data indicated that the main effect of diet and genotype on PSD-95 was not statistically significant. However, there was a significant interaction between the effects of diet and the genotype on PSD-95 level (* $p < 0.05$). Post-hoc analysis showed that the PSD-95 expression level was significantly increased in C57BL/6 mice with the Western diet compared to chow diet (* $p < 0.05$) (Figure 3.5). There was no change in the PSD-95 protein level in ApoE^{-/-} mice with both chow and Western diet. PSD-95 protein levels were significantly higher in ApoE^{-/-} mice than C57BL/6 with chow diet (* $p < 0.05$) (Figure 3.5). Western diet did not change the PSD-95 expression level in both strains.

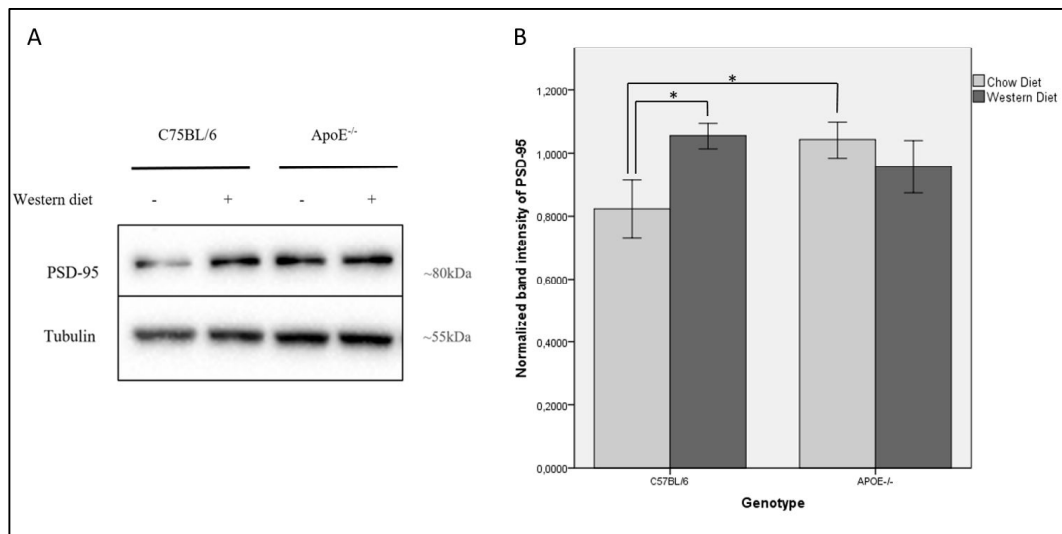


Figure 3.5. The Western blot analysis of PSD-95 in the hippocampus. (A) Representative immunoblot and (B) the quantification of the immunoblots (n=7, biological replicates) (n=3, technical replicates). Each bar represents Mean ± SEM. Dark grey showed Western diet fed animals and light grey showed chow diet fed animals. (*p<0.05)

3.1.4. Neurogenesis

To determine neurogenesis DCX, an immature neuronal marker was used [90]. Two-way ANOVA analysis showed that the main effect of diet on the DCX levels were not significant but the main effect of genotype on DCX was significant (**p<0.001). Nevertheless, post-hoc analysis relieved that the DCX expression levels have a tendency to increase in ApoE^{-/-} mice (p=0.052) with Western diet compared to chow diet. Additionally, the DCX levels were significantly higher in ApoE^{-/-} strain than C57BL/6 strain with both Western diet (**p<0.001) and chow diet (*p<0.05) (Figure3.6).

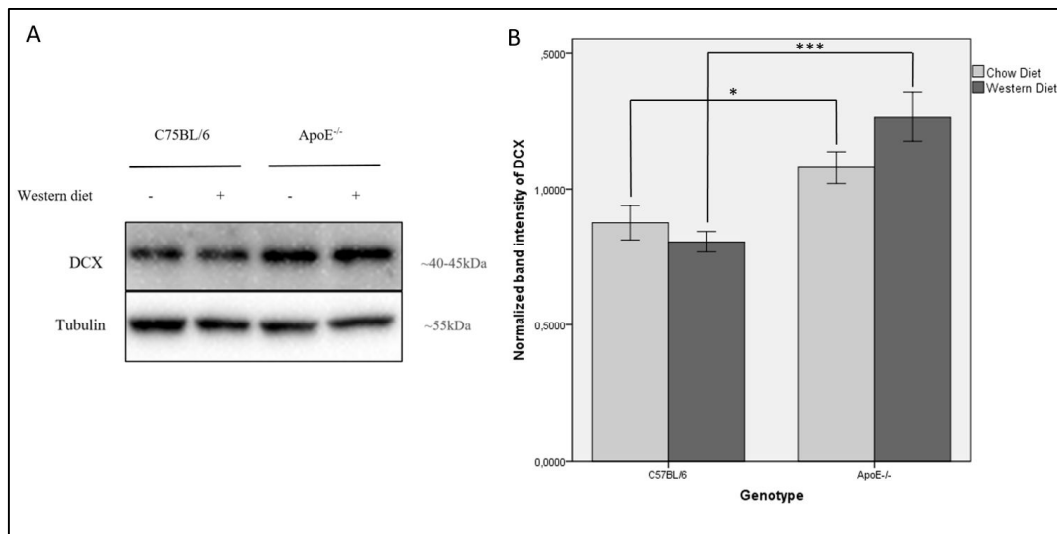


Figure 3.6. The Western blot analysis of DCX in the hippocampus. (A) Representative immunoblot and (B) the quantification of the immunoblots (n=7, biological replicates) (n=3, technical replicates). Each bar represents Mean ± SEM. Dark grey showed Western diet fed animals and light grey showed chow diet fed animals. (* $p < 0.05$, *** $p < 0.001$)

3.2. The effects of Western Diet on the Cerebral Cortex

3.2.1. ER Stress

3.2.1.1. p-PERK

There was a significant genotype effect on p-PERK levels in the cerebral cortex, nevertheless, the effect of diet was not detected. p-PERK levels of C57BL/6 mice were statistically significantly elevated with Western diet compared to chow diet (* $p < 0.05$) (Figure 3.7). Also, p-PERK levels was significantly higher in ApoE^{-/-} compared to C57BL/6 mice when they fed with chow diet (* $p < 0.05$) (Figure 3.7).

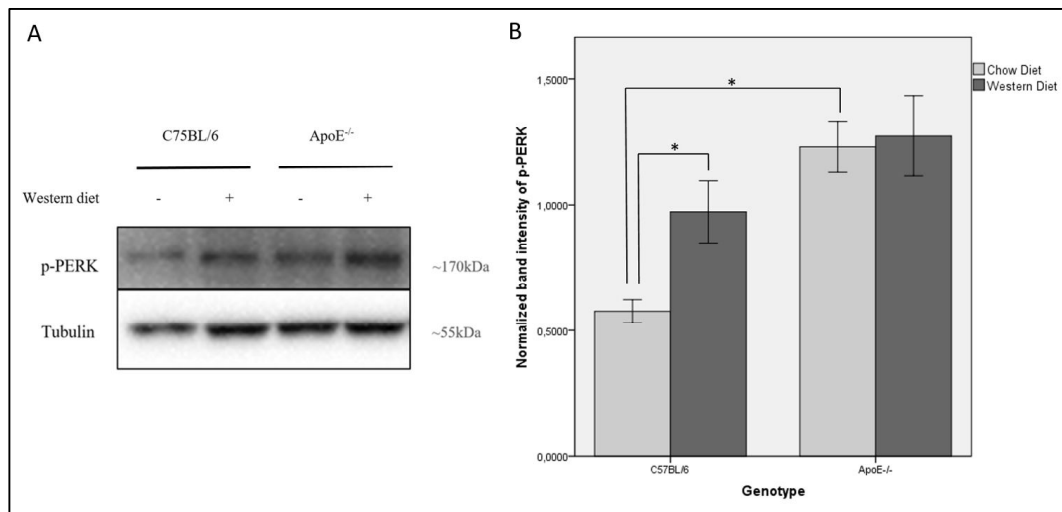


Figure 3.7. The Western blot analysis of p-PERK in the cerebral cortex [88]. (A) Representative immunoblot and (B) the quantification of the immunoblots (n=7, biological replicates) (n=2, technical replicates). Each bar represents Mean ± SEM. Dark grey showed Western diet fed animals and light grey showed chow diet fed animals. (* $p < 0.05$)

3.2.1.2. p-eIF2 α

Data revealed that diet (* $p < 0.05$) and the genotype (** $p < 0.001$) had an impact on p-eIF2 α protein levels. In both Western diet (** $p < 0.001$) and chow diet groups (** $p < 0.001$), p-eIF2 α expression levels were higher in ApoE^{-/-} mice than C57BL/6 mice (Figure 3.8). Furthermore, the p-eIF2 α protein level was increased in C57BL/6 strain with Western diet compared to chow diet (* $p < 0.05$) (Figure 3.8).

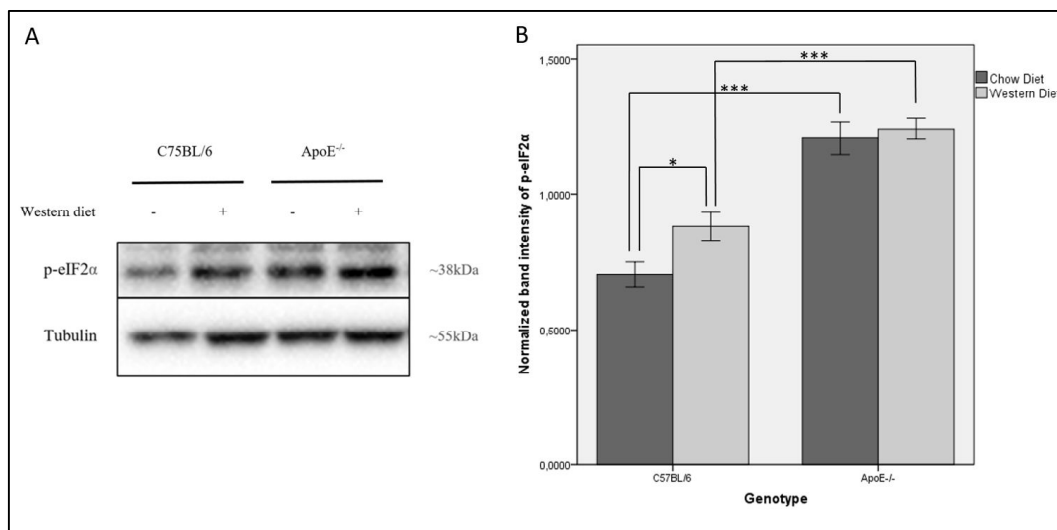


Figure 3.8. The Western blot analysis of p-eIF2 α in the cerebral cortex. (A) Representative immunoblot and (B) the quantification of the immunoblots (n=7, biological replicates) (n=3, technical replicates). Each bar represents Mean \pm SEM. Dark grey showed Western diet fed animals and light grey showed chow diet fed animals. (*p<0.05, ***p<0.001)

3.2.1.3. CHOP

There was a significant main effect of genotype (**p<0.01) on CHOP levels but the main effect of diet was not detected on CHOP expression. Post-hoc analysis showed that when they had given chow diet, the expression of CHOP was increased in ApoE^{-/-} mice compared to C57BL/6 (**p<0.01) (Figure 3.9).

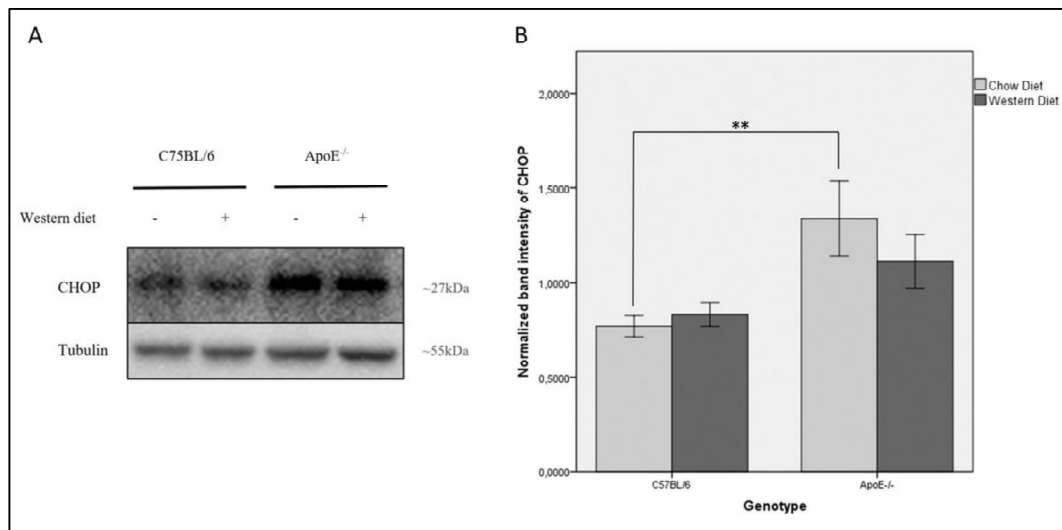


Figure 3.9. The Western blot analysis of CHOP in the cerebral cortex. (A) Representative immunoblot and (B) the quantification of the immunoblots (n=7, biological replicates) (n=2, technical replicates). Each bar represents Mean ± SEM. Dark grey showed Western diet fed animals and light grey showed chow diet fed animals. (**p<0.01)

3.2.2. Inflammation

Although the effect of diet on IL-1 beta levels were not significant, the effect of genotype on IL-1 beta levels were significant. In ApoE^{-/-} mice IL-1 beta levels were significantly higher than C57BL/6 mice (*p<0.05) (Figure 3.10).

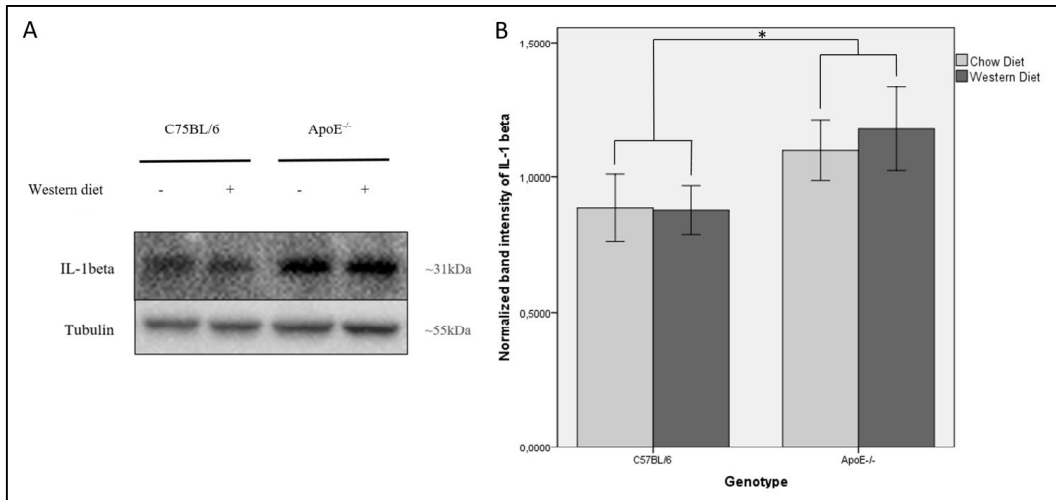


Figure 3.10. The Western blot analysis of IL-1 beta in the cerebral cortex. (A) Representative immunoblot and (B) the quantification of the immunoblots (n=7, biological replicates) (n=2, technical replicates). Each bar represents Mean \pm SEM. Dark grey showed Western diet fed animals and light grey showed chow diet fed animals. (* p <0.05)

3.2.3. Postsynaptic Integrity

There was a significant effect of genotype on PSD-95 expression levels in cerebral cortex (* p <0.05) (Figure 3.11). In ApoE^{-/-} mice chow diet had a tendency to increase the PSD-95 levels compared to C57BL/6 strain (p =0.059).

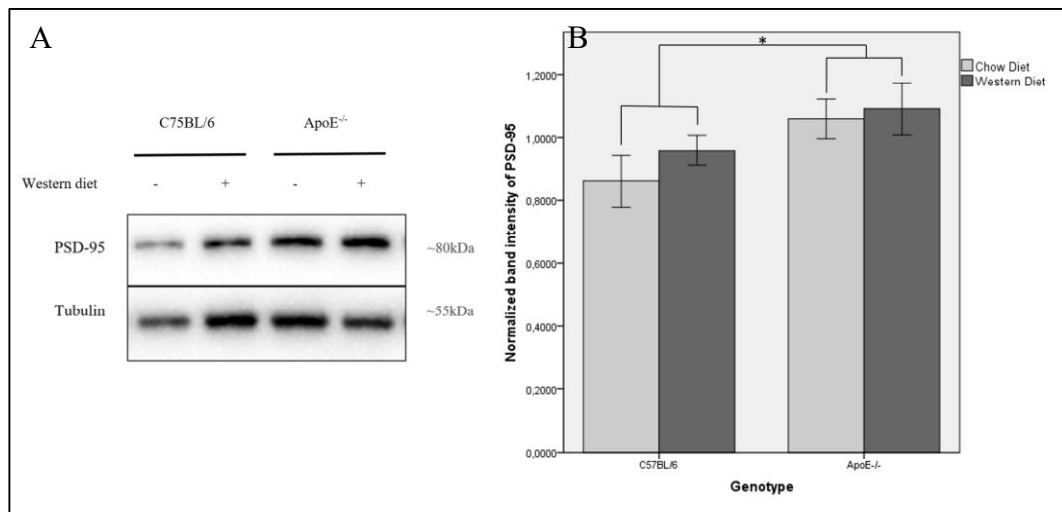


Figure 3.11. The Western blot analysis of PSD-95 in the cerebral cortex. (A) Representative immunoblot and (B) the quantification of the immunoblots (n=7, biological replicates) (n=3, technical replicates). Each bar represents Mean ± SEM. Dark grey showed Western diet fed animals and light grey showed chow diet fed animals. (* $p < 0.05$)

3.2.4. Neurogenesis

There was a significant main effect of both diet (* $p < 0.05$) and genotype (** $p < 0.001$) on DCX expression. Further interaction analysis showed significantly increased DCX protein levels in ApoE^{-/-} mice compared to C57BL/6 upon the chow diet (** $p < 0.001$) (Figure 3.12). The DCX expression also was higher in ApoE^{-/-} strain in comparison to C57BL/6 genotype with the Western diet (** $p < 0.001$) (Figure 3.12).

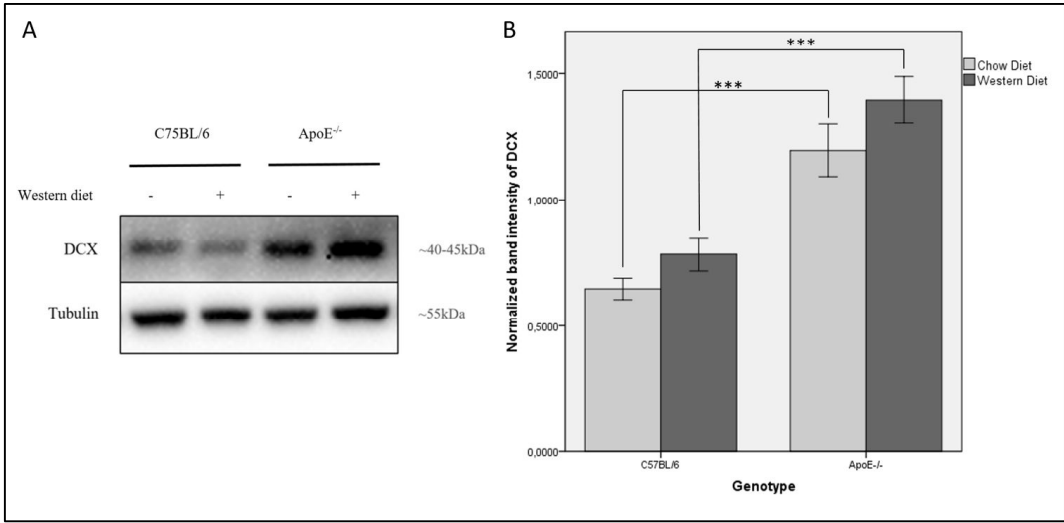


Figure 3.12. The Western blot analysis of DCX in the cerebral cortex. (A) Representative immunoblot and (B) the quantification of the immunoblots ((n=7, biological replicates) (n=3, technical replicates)). Each bar represents Mean ± SEM. Dark grey showed Western diet fed animals and light grey showed chow diet fed animals. (***) $p < 0.001$

3.3. IHC Optimization

NeuN was used for the identification of mature neurons in brain sections [91]. The optimization results of IHC for different dilutions (1:2000, 1:4000, 1:8000) of NeuN were given in Figure 3.13, Figure 3.14, Figure 3.15. In order to capture images with higher quality to be able to count the neurons, the permeabilization process was performed Figure 3.16.

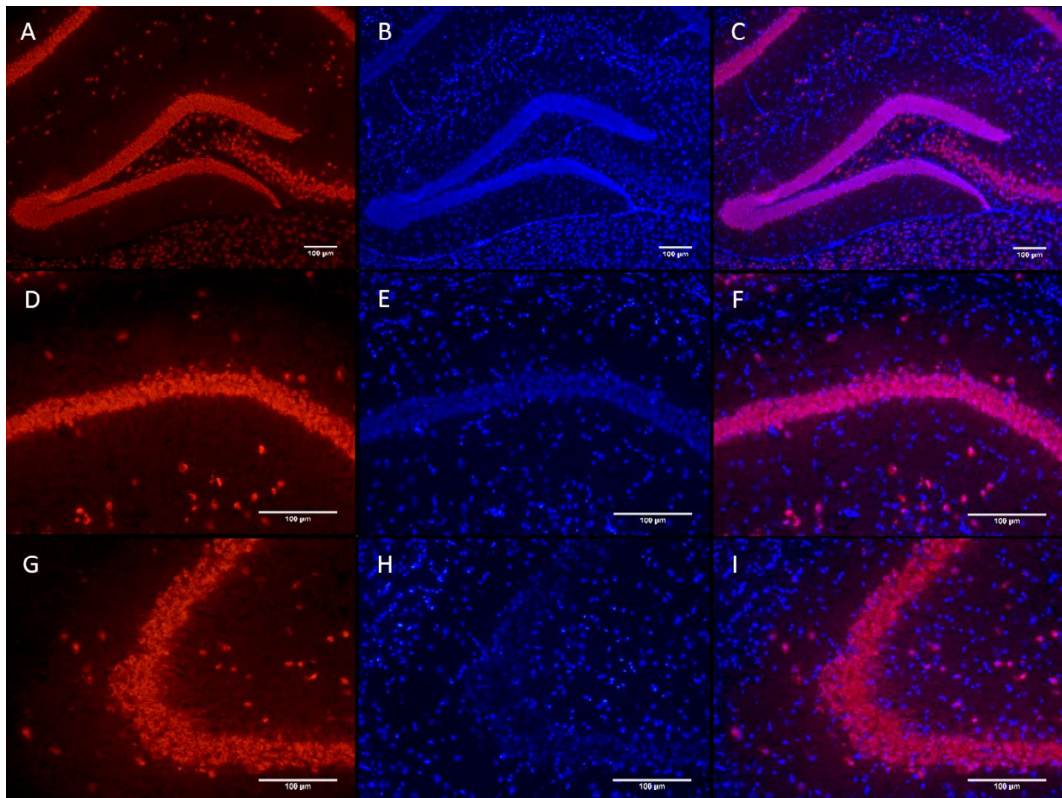


Figure 3.13. The immunofluorescence staining of the hippocampus with 1:2000 NeuN. Red fluorescence was NeuN (1:2000), blue fluorescence was DAPI marker and NeuN+DAPI (C, F, I). DG region at 10X magnification (A, B, and C), CA1 region at 20X magnification (D, E, and F), CA3 region at 20X magnification (G, H, and I). DG: Dentate gyrus, CA: Cornu ammonis. The images were captured via Zeiss fluorescent microscope (Axio Zoom.V16, Zeiss, Oberkochen, Germany, UNAM, Bilkent University).

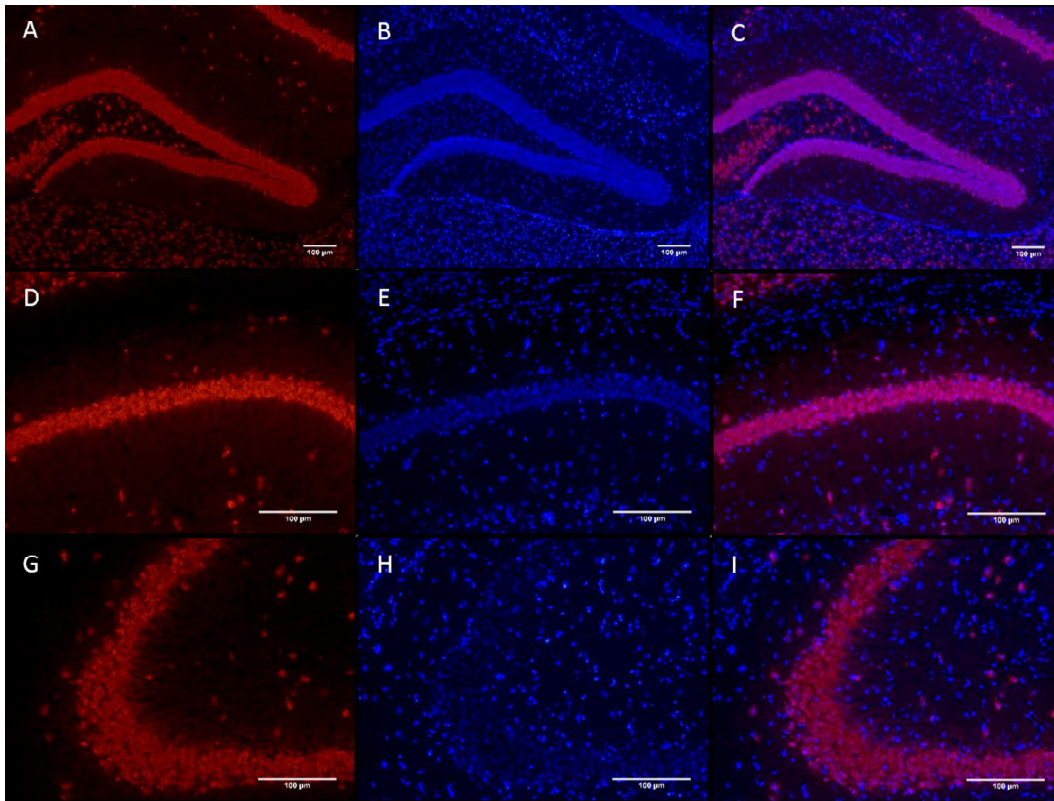


Figure 3.14. The immunofluorescence staining of the hippocampus with 1:4000 NeuN. Red fluorescence was NeuN (1:4000), blue fluorescence was DAPI marker and NeuN+DAPI (C, F, I). DG region at 10X magnification (A, B, and C), CA1 region at 20X magnification (D, E, and F), CA3 region at 20X magnification (G, H, and I). DG: Dentate gyrus, CA: Cornu ammonis. The images were captured via Zeiss fluorescent microscope (Axio Zoom.V16, Zeiss, Oberkochen, Germany, UNAM, Bilkent University).

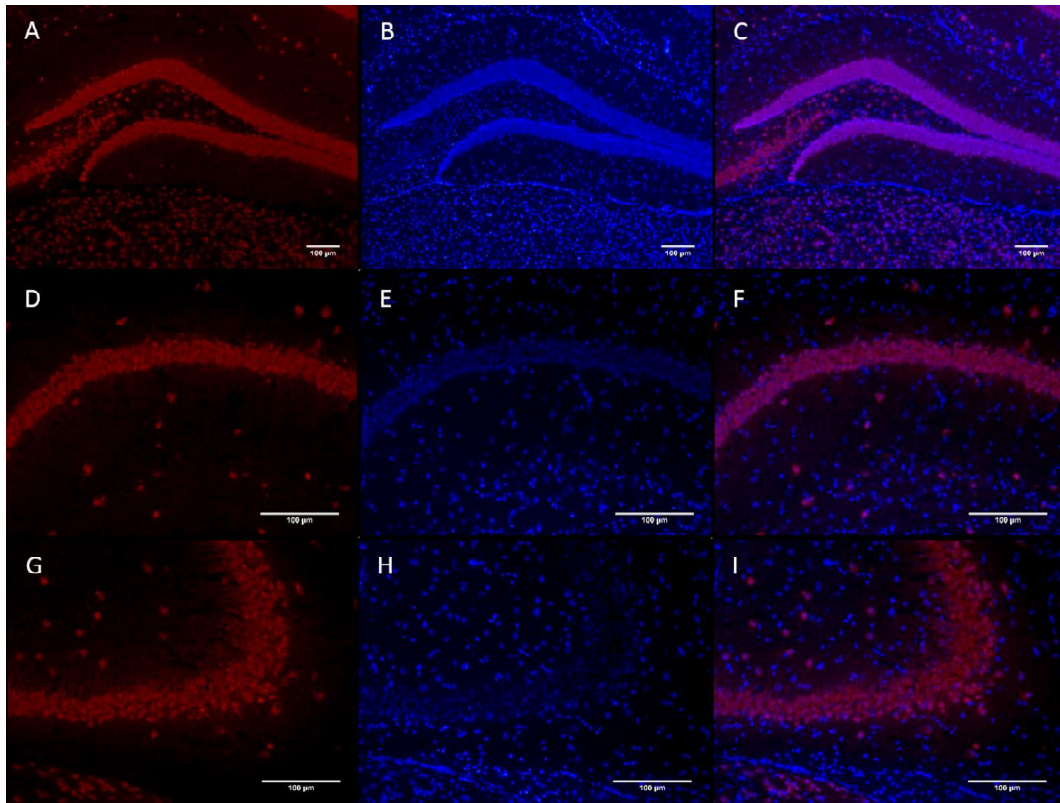


Figure 3.15. The immunofluorescence staining of the hippocampus with 1:8000 NeuN. Red fluorescence was NeuN (1:8000), blue fluorescence was DAPI marker and NeuN+DAPI (C, F, I). DG region at 10X magnification (A, B, and C), CA1 region at 20X magnification (D, E, and F), CA3 region at 20X magnification (G, H, and I). DG: Dentate gyrus, CA: Cornu ammonis. The images were captured via Zeiss fluorescent microscope (Axio Zoom.V16, Zeiss, Oberkochen, Germany, UNAM, Bilkent University).

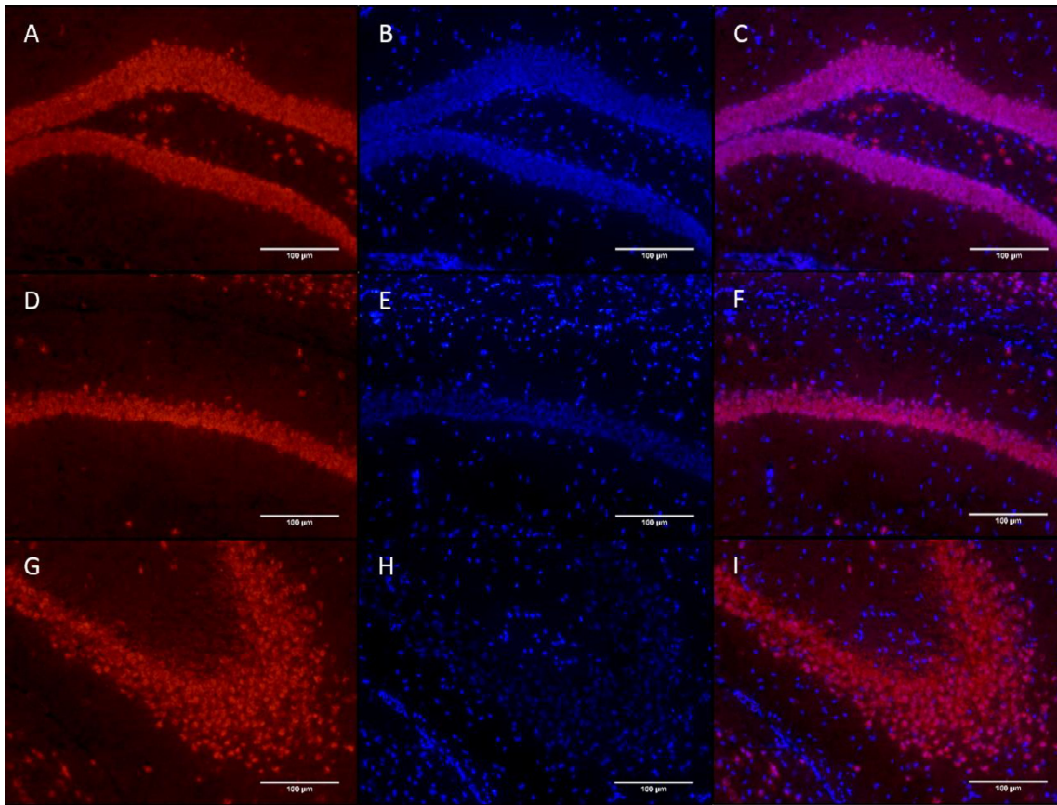


Figure 3.16. The immunofluorescence staining of the hippocampus with NeuN in permeabilized sections. Red fluorescence was NeuN (1:4000), blue fluorescence was DAPI marker and NeuN+DAPI (C, F, I). DG region at 20X magnification (A, B, and C), CA1 region at 20X magnification (D, E, and F), CA3 region at 20X magnification (G, H, and I). DG: Dentate gyrus, CA: Cornu ammonis. The images were captured via Zeiss fluorescent microscope (Axio Zoom.V16, Zeiss, Oberkochen, Germany, UNAM, Bilkent University).

The images of IL-1 beta by optimized IHC method were given Figure 3.17.

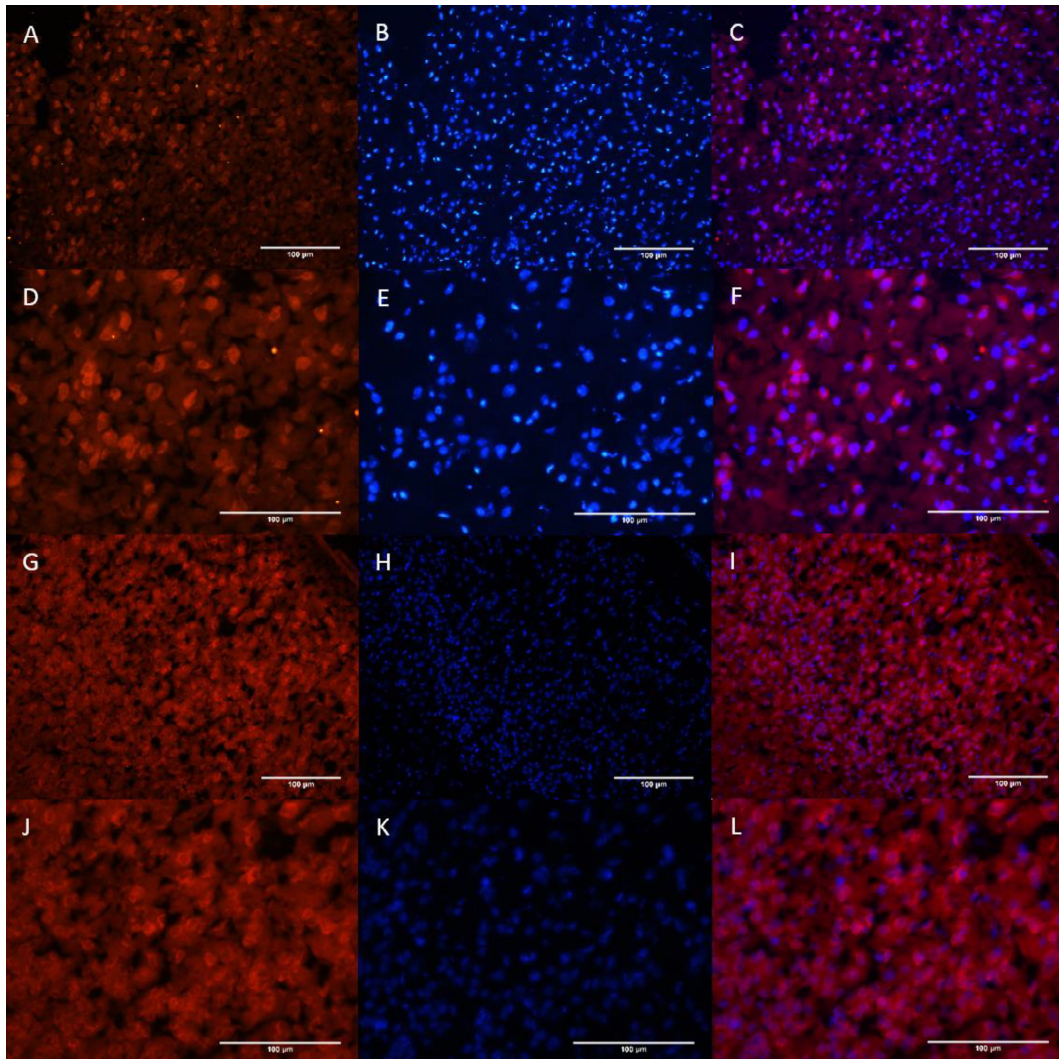


Figure 3.17. The immunofluorescence staining of the cerebral cortex and hypothalamus with IL-1 beta. Red fluorescence was IL-1 beta (1:150), blue fluorescence was DAPI marker and IL-1 beta+DAPI (C, F, I, and L). Cerebral cortex region at 20X magnification (A, B, and C), at 40X magnification (D, E and F), Hypothalamus region at 20X magnification (G, H, and I), at 40X magnification (J, K, and L). The images were captured via Zeiss fluorescent microscope (Axio Zoom.V16, Zeiss, Oberkochen, Germany, UNAM, Bilkent University).

The images of active Caspase-1 by optimized IHC method were given Figure 3.17.

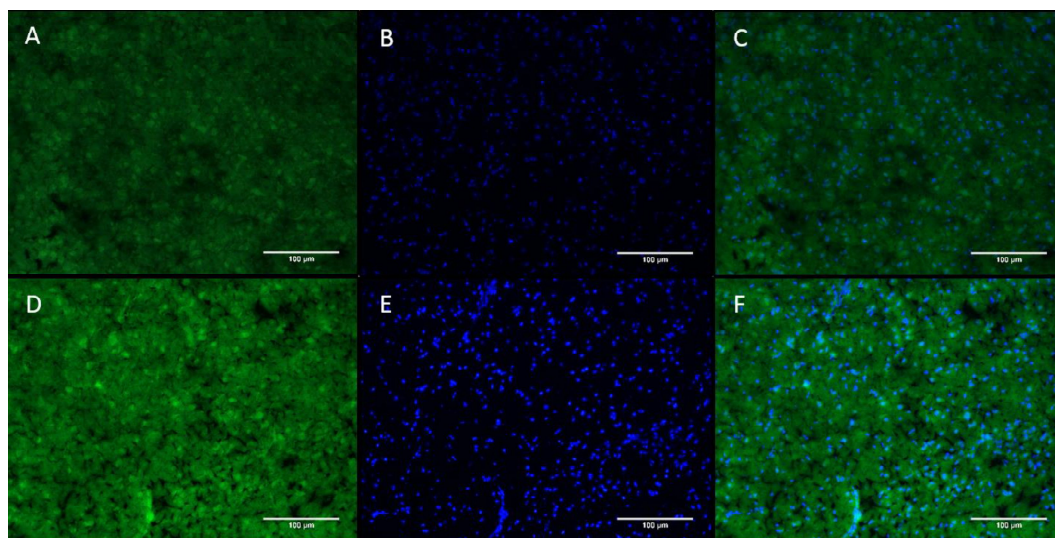


Figure 3.18. The immunofluorescence staining of the cerebral cortex with **Caspase-1**. Green fluorescence was active Caspase-1, blue fluorescence was DAPI marker and Caspase-1+DAPI (C, F, I). Cerebral cortex region at 20X magnification (1:300) (A, B, and C), cerebral cortex region at 20X magnification (1:150) (D, E, and F). The images were captured via Zeiss fluorescent microscope (Axio Zoom.V16, Zeiss, Oberkochen, Germany, UNAM, Bilkent University).

CHAPTER 4

DISCUSSION

Diet including high-fat content has been associated with hippocampal-dependent memory and cognitive impairments [92]. Neuroinflammation is considered as a potential cause behind these deficits. Elevated serum lipid levels lead to alterations in BBB resulting in higher permeability of the structure [93]. It was suggested that this can make hippocampus more prone to the effects of diet-induced neuroinflammation. In these studies, inflammation was accompanied with decreased synaptic integrity and increased in markers used for apoptosis, pointing out a potential neuronal loss [52]. The PERK pathway is one of the branches of ER stress and is induced with HFD. The activation of the PERK pathway resulting in attenuation of global protein synthesis and selective translation of proteins involved in apoptosis and inflammatory response [66]. Since the effects of HFD in neurons resemble the results of stimulated PERK pathway, the idea of manipulation of this pathway as a therapeutic approach has been promising recently. GSK, Sephin 1 and ISRIB are different inhibitors of PERK pathway, they have been used in neurodegenerative diseases and found to enhance the pathological conditions of these diseases [94].

In this study by using ApoE^{-/-} mice fed with HC/HFD as a hyperlipidemic animal model, how Western diet alters neurons in different respects and affects the ER stress in the hippocampus and the cerebral cortex were investigated. The immunoblot analysis of markers was assessed to show ER stress, inflammation, synaptic integrity and neurogenesis in the subjects.

Previous studies showed HFD results in the induction of the PERK pathway and elevated inflammation in the hippocampus of mice [74]. Therefore, our hypothesis was to observe an increase in PERK pathway markers. Yet, in our study, there were

no significant differences of p-PERK, p-eIF2 α levels in the hippocampus and surprisingly there was a decline in CHOP, IL-1 beta levels with Western diet in both strains. Simultaneous decrease of CHOP and inflammation marker supports the consistency of our results. It is necessary to analyze the levels of other cytokines such as TNF-alpha to confirm the decrease in inflammation. To understand why there is a decrease in the protein levels of CHOP and IL-1beta, further studies should be performed.

Additionally, the studies revealed a correlation between high TC levels and cognitive impairment in mid to old aged humans [95]. In our study, subjects were 25 weeks old and are considered mature young adults [96] which might be the reason why inflammation and apoptosis were not detected in their hippocampi. PSD-95 was used to examine the excitatory postsynaptic integrity of the neurons. Since several studies found a decline in PSD-95 levels with HFD, lower PSD-95 levels were expected in the hippocampus of hyperlipidemic mice [97]. Yet, PSD-95 was significantly increased with the Western diet in C57BL/6 group and no effect was detected in the ApoE^{-/-} group. The absence of ER stress and decreased inflammation might be the reason why we did not observe a decrease in PSD-95 for Western diet groups in our study.

Similar to the hippocampus, it was expected to detect an increase in PERK pathway markers accompanied by inflammation in the cerebral cortex of the mice fed with the Western diet. In the cerebral cortex, the impact of genotype on p-PERK and p-eIF2 α was significant, these markers were higher in ApoE^{-/-} mice. Our results suggested a potential diet-induced activation of the PERK pathway in the control group, whereas in ApoE^{-/-} mice the difference was not induced by the diet. Similarly, CHOP, IL-1 beta, and PSD-95 levels were higher in ApoE^{-/-} mice but the diet did not affect the CHOP, IL-1 beta, and PSD-95 levels. The literature points out that the plasma cholesterol was mainly carried on HDL in wild-type mice on regular chow diet and their LDL levels were lower than humans. Even if they were fed with Western diet, these mice show high HDL/LDL ratio so that they are highly resistant to the

development of atherosclerosis [98]. Therefore, this group only shows the consequences of high cholesterol diet (HCD). HCD and hyperlipidemia induced the PERK pathway, whereas apoptotic, inflammatory and postsynaptic integrity markers only increased by ApoE^{-/-} genotype and they were not altered by HCD. The effect of diet on ApoE^{-/-} subjects was not detected. As mentioned in the introduction, ApoE protein functions as a ligand for the uptake of CM and VLDL and their remnants to LDL, its absence causes the slow clearance of lipoproteins and results in hypocholesteremia and atherosclerotic lesions even if they are fed with a chow diet [98]. Consequently, this genotype effect with chow diet can be the reason why the alterations caused by the Western diet were not detected in ApoE^{-/-} mice. Absence of a decrease in PSD-95 levels may indicate that postsynaptic integrity was not affected by the induced PERK pathway. However, the isolation of proteins was performed from cerebral cortex tissue directly. In order to assess the results more accurately, synaptic proteins in synaptosomes can be isolated and analyzed, or inhibitory synaptic proteins may be studied to comprehend whether the balance between excitatory and inhibitory synaptic proteins was disrupted.

It was hypothesized to observe lower DCX levels with the Western diet since lower BDNF levels were documented with HFD [59]. Our study showed a significant rise in immature neurogenesis marker in ApoE^{-/-} mice compared to C57BL/6 strain, suggesting a potential genotype effect on neurogenesis as also observed in another research by Janssen, et. al (2016). They used 12 months-old mice fed with HFD (19% butter, 0.5% cholate, 1.25% cholesterol) for 3 months and did not detect any changes in DCX levels [99]. Higher DCX levels is an indicator of more neurons, nevertheless, detecting only DCX levels may not show whether the neurons are going to survive and become mature neurons. Hence, a mature neuronal marker such as NeuN was used to validate the neuron numbers. So as to achieve this goal, the optimization of NeuN was performed with IHC (Figure 3.13, Figure 3.14 and Figure 3.15). The quality of images was not sufficient enough to count the neurons one by one. The neurons were densely distributed in hippocampal regions. Although permeabilization method makes

counting of neurons in CA1 and CA3 regions possible, we were not able to count the neurons in the DG region (Figure 3.16). Nissl staining is a histological method used for staining of neurons. It has been widely used to analyze the morphology and pathology of neurons [100], [101]. Therefore, Nissl staining can be assessed in future studies. The optimization of IHC of IL-1beta and caspase-1 was shown in Figure 3.17 and Figure 3.18. The analysis of IL-1beta can help us with confirming the accuracy of decreased levels of this inflammation marker in the hippocampus and increased levels of this inflammation marker in the cerebral cortex of ApoE^{-/-} mice. IHC results of caspase-1 would support us to investigate whether there is an increase in inflammation-induced neuronal death in both brain regions. Additionally, since there is an activation PERK pathway in the cerebral cortex of ApoE^{-/-} subjects, IHC analysis of these markers on the cerebral cortex of the subjects would show us whether using PERK pathway inhibitors will diminish the inflammation and the cell death induced by inflammation in the cerebral cortex.

CHAPTER 5

CONCLUSION AND FUTURE DIRECTIONS

In this study, the impacts of HC/HFD on ER stress, inflammation, postsynaptic integrity, and neurogenesis were analyzed in the hippocampus and the cerebral cortex in ApoE^{-/-} and C57BL/6 mice. ApoE^{-/-} strain was used as a hyperlipidemic animal model and C57BL/6 mice were used as a control group. Experiments were initiated with 8 weeks old male mice and diet lasted for 16 weeks.

Our results showed that diet and the genotype did not induce the PERK pathway in the hippocampus. Essentially, CHOP and IL-1 beta levels were decreased with the Western diet in both strains suggesting HC/HFD might diminish inflammation in this region. Diet did not alter the PSD-95 levels in the hippocampus suggesting there would be no decrease in postsynaptic integrity in hippocampal neurons of hyperlipidemic mice. Western blot analyses suggested that the genotype significantly altered the levels of PERK pathway, inflammation, and postsynaptic integrity markers in the cerebral cortex, whereas diet did not make a difference in protein levels of PSD-95. The ER stress markers were higher in ApoE^{-/-} mice than C57BL/6 mice. Since IL-1 beta and PSD-95 were also elevated in the ApoE^{-/-} group. Higher neurogenesis was detected in both the hippocampus and the cerebral cortex of ApoE^{-/-} mice.

As future studies, IHC will be performed to observe whether the PERK inhibitors change the high cholesterol-induced alterations in the hippocampus and in the cortex. To confirm decreased inflammation, other cytokines such as TNF-alpha and IL-6 might be assessed in the hippocampus. To study synaptic integrity, inhibitory synaptic proteins would be checked to whether the balance between inhibitory and excitatory synapses was disrupted. Moreover, performing synaptosome isolation and assessing synaptic proteins from synaptosomes would be a better approach to study synaptic integrity. Since human studies correlated cognitive deficits with high TC levels at mid-

life, middle-aged mice would be used to mimic this correlation in hyperlipidemia studies.

REFERENCES

- [1] F. Ofei, "Obesity - a preventable disease," *Ghana Med. J.*, vol. 39, no. 3, pp. 98–101, Sep. 2005.
- [2] R. T. Hurt, C. Kulisek, L. A. Buchanan, and S. A. McClave, "The obesity epidemic: challenges, health initiatives, and implications for gastroenterologists," *Gastroenterol. Hepatol. (N. Y.)*, vol. 6, no. 12, pp. 780–92, Dec. 2010.
- [3] The Organization for Economic Co-operation and Development (OECD) Health Statistics., "Policy insights," 2017. [Online]. Available: www.oecd.org/health/obesity-update.htm. [Accessed: 14-Jun-2019].
- [4] R. H. Nelson, "Hyperlipidemia as a risk factor for cardiovascular disease," *Prim. Care*, vol. 40, no. 1, pp. 195–211, Mar. 2013.
- [5] World Health Organization, "Cardiovascular diseases (CVDs)," 2017. [Online]. Available: [https://www.who.int/en/news-room/factsheets/detail/cardiovascular-diseases-\(cvds\)](https://www.who.int/en/news-room/factsheets/detail/cardiovascular-diseases-(cvds)). [Accessed: 09-Jun-2019].
- [6] World Health Organization, "*Noncommunicable Diseases Country Profiles 2018*," vol. 369, no. 14. 2018.
- [7] The Emerging Risk Factors Collaboration* *et al.*, "Major Lipids, Apolipoproteins, and Risk of Vascular Disease," *JAMA*, vol. 302, no. 18, p. 1993, Nov. 2009.
- [8] R. A. Cox and M. R. García-Palmieri, "*Cholesterol, Triglycerides, and Associated Lipoproteins*," *Butterworths*, 1990.

- [9] N. Rifai, P. S. Bachorik, J. J. Albers, “Lipids, Lipoproteins and apolipoproteins,” 3rd ed. *Philadelphia: wb saunders company*, 1999, pp. 809–861.
- [10] K. R. Feingold and C. Grunfeld, “Introduction to Lipids and Lipoproteins,” MDText.com, Inc., 2000.
- [11] X. Pan and M. M. Hussain, “Gut triglyceride production,” *Biochim. Biophys. Acta - Mol. Cell Biol. Lipids*, vol. 1821, no. 5, pp. 727–735, May 2012.
- [12] S. W. Altmann *et al.*, “Niemann-Pick C1 Like 1 Protein Is Critical for Intestinal Cholesterol Absorption,” *Science (80)*, vol. 303, no. 5661, pp. 1201–1204, Feb. 2004.
- [13] B. Klop, J. W. Jukema, T. J. Rabelink, M. Castro Cabezas “A physician’s guide for the management of hypertriglyceridemia: The etiology of hypertriglyceridemia determines treatment strategy,” *Panminerva Med.*, 2012, pp.91–103.
- [14] J. B. Dixon, “Mechanisms of chylomicron uptake into lacteals,” *Ann. N. Y. Acad. Sci.*, vol. 1207, pp. E52–E57, Oct. 2010.
- [15] Ž. Reiner, “Triglyceride-Rich Lipoproteins and Novel Targets for Anti-atherosclerotic Therapy.,” *Korean Circ. J.*, vol. 48, no. 12, pp. 1097–1119, Dec. 2018.
- [16] R. W. Mahley and Z. S. Ji, “Remnant lipoprotein metabolism: key pathways involving cell-surface heparan sulfate proteoglycans and apolipoprotein E,” *J. Lipid Res.*, vol. 40, no. 1, pp. 1–16, Jan. 1999.
- [17] N. A. Abumrad and N. O. Davidson, “Role of the Gut in Lipid Homeostasis,” *Physiol. Rev.*, vol. 92, no. 3, pp. 1061–1085, Jul. 2012.

- [18] W. Yang, H. Shi, J. Zhang, Z. Shen, G. Zhou, and M. Hu, “Effects of the duration of hyperlipidemia on cerebral lipids, vessels and neurons in rats,” *Lipids Health Dis.*, vol. 16, no. 1, p. 26, Jan. 2017.
- [19] J. Banefelt *et al.*, “Work productivity loss and indirect costs associated with new cardiovascular events in high-risk patients with hyperlipidemia: estimates from population-based register data in Sweden,” *Eur. J. Heal. Econ.*, vol. 17, no. 9, pp. 1117–1124, Dec. 2016.
- [20] N. E. Shepardson, G. M. Shankar, and D. J. Selkoe, “Cholesterol Level and Statin Use in Alzheimer Disease,” *Arch. Neurol.*, vol. 68, no. 10, p. 1239, Oct. 2011.
- [21] R. M. Adibhatla and J. F. Hatcher, “Altered Lipid Metabolism in Brain Injury and Disorders,” in *Lipids in Health and Disease*, Dordrecht: Springer Netherlands, pp. 241–268.
- [22] L. M. Hinder, A. M. Vincent, J. M. Hayes, L. L. McLean, and E. L. Feldman, “Apolipoprotein E knockout as the basis for mouse models of dyslipidemia-induced neuropathy,” *Exp. Neurol.*, vol. 239, pp. 102–110, Jan. 2013.
- [23] K. S. Meir and E. Leitersdorf, “Atherosclerosis in the Apolipoprotein E–Deficient Mouse,” *Arterioscler. Thromb. Vasc. Biol.*, vol. 24, no. 6, pp. 1006–1014, Jun. 2004.
- [24] A. A. Pendse, J. M. Arbones-Mainar, L. A. Johnson, M. K. Altenburg, and N. Maeda, “Apolipoprotein E knock-out and knock-in mice: atherosclerosis, metabolic syndrome, and beyond,” *J. Lipid Res.*, vol. 50 Suppl, no. Suppl, pp. S178-82, Apr. 2009.
- [25] J. Poirier, “Apolipoprotein E and Alzheimer’s Disease A Role in Amyloid Catabolism,” *Ann. N. Y. Acad. Sci.*, vol. 924, no. 1, pp. 81–90, Jan. 2006.

- [26] P. B. Gorelick, "Role of inflammation in cognitive impairment: results of observational epidemiological studies and clinical trials," *Ann. N. Y. Acad. Sci.*, vol. 1207, no. 1, pp. 155–162, Oct. 2010.
- [27] M. F. Gregor and G. S. Hotamisligil, "Inflammatory Mechanisms in Obesity," *Annu. Rev. Immunol.*, vol. 29, no. 1, pp. 415–445, Apr. 2011.
- [28] J. C. D. Nguyen, A. S. Killcross, and T. A. Jenkins, "Obesity and cognitive decline: role of inflammation and vascular changes," *Front. Neurosci.*, vol. 8, p. 375, Nov. 2014.
- [29] X. Shu *et al.*, "Extracts of *Salvia-Nelumbinis Naturalis* Ameliorate Nonalcoholic Steatohepatitis via Inhibiting Gut-Derived Endotoxin Mediated TLR4/NF- κ B Activation.," *Evid. Based. Complement. Alternat. Med.*, vol. 2017, p. 9208314, 2017.
- [30] K. Honda and T. Taniguchi, "IRFs: master regulators of signalling by Toll-like receptors and cytosolic pattern-recognition receptors," *Nat. Rev. Immunol.*, vol. 6, no. 9, pp. 644–658, Sep. 2006.
- [31] M. Gros Lambert and B. F. Py, "Spotlight on the NLRP3 inflammasome pathway," *J. Inflamm. Res.*, vol. 11, pp. 359–374, 2018.
- [32] J. P. Thaler, S. J. Guyenet, M. D. Dorfman, B. E. Wisse, and M. W. Schwartz, "Hypothalamic Inflammation: Marker or Mechanism of Obesity Pathogenesis?," *Diabetes*, vol. 62, no. 8, pp. 2629–2634, Aug. 2013.
- [33] N. J. Abbott and A. Friedman, "Overview and introduction: The blood-brain barrier in health and disease," *Epilepsia*, vol. 53, pp. 1–6, Nov. 2012.
- [34] L. M. Williams, "Hypothalamic dysfunction in obesity," *Proc. Nutr. Soc.*, vol. 71, no. 4, pp. 521–533, Nov. 2012.

- [35] S. Kälin, F. L. Heppner, I. Bechmann, M. Prinz, M. H. Tschöp, and C.-X. Yi, "Hypothalamic innate immune reaction in obesity," *Nat. Rev. Endocrinol.*, vol. 11, no. 6, pp. 339–351, Jun. 2015.
- [36] Y. Tang, S. Purkayastha, and D. Cai, "Hypothalamic microinflammation: a common basis of metabolic syndrome and aging," *Trends Neurosci.*, vol. 38, no. 1, pp. 36–44, Jan. 2015.
- [37] E. Elwood, Z. Lim, H. Naveed, and I. Galea, "The effect of systemic inflammation on human brain barrier function," *Brain. Behav. Immun.*, vol. 62, pp. 35–40, May 2017.
- [38] C. M. Blatteis, "The onset of fever: new insights into its mechanism," in *Progress in brain research*, vol. 162, 2007, pp. 3–14.
- [39] P. Lu *et al.*, "CNS penetration of small molecules following local inflammation, widespread systemic inflammation or direct injury to the nervous system," *Life Sci.*, vol. 85, no. 11–12, pp. 450–456, Sep. 2009.
- [40] A. Patel and J. B. Fowler, "Neuroanatomy, Temporal Lobe," *StatPearls Publishing*, 2019.
- [41] M. Seghatoleslam *et al.*, "The effects of *Nigella sativa* on neural damage after pentylenetetrazole induced seizures in rats," *J. Tradit. Complement. Med.*, vol. 6, no. 3, pp. 262–268, Jul. 2016.
- [42] V. Dhikav and K. Anand, "Hippocampus in health and disease: An overview," *Ann. Indian Acad. Neurol.*, vol. 15, no. 4, p. 239, Oct. 2012.
- [43] B. T. Giap, C. N. Jong, J. H. Ricker, N. K. Cullen, and R. D. Zafonte, "The hippocampus: anatomy, pathophysiology, and regenerative capacity," *J. Head Trauma Rehabil.*, vol. 15, no. 3, pp. 875–94, Jun. 2000.

- [44] Y. Taki *et al.*, “Relationship Between Body Mass Index and Gray Matter Volume in 1,428 Healthy Individuals,” *Obesity*, vol. 16, no. 1, pp. 119–124, Jan. 2008.
- [45] C. A. Raji *et al.*, “Brain structure and obesity,” *Hum. Brain Mapp.*, vol. 31, no. 3, p. NA-NA, Mar. 2009.
- [46] S. Gazdzinski, J. Kornak, M. W. Weiner, and D. J. Meyerhoff, “Body mass index and magnetic resonance markers of brain integrity in adults,” *Ann. Neurol.*, vol. 63, no. 5, pp. 652–657, May 2008.
- [47] P. van Vliet, “Cholesterol and Late-Life Cognitive Decline,” *J. Alzheimer’s Dis.*, vol. 30, no. s2, pp. S147–S162, Jun. 2012.
- [48] D. M. Abo El-Khair, F. E.-N. A. El-Safti, H. Z. Nooh, and A. E. El-Mehi, “A comparative study on the effect of high cholesterol diet on the hippocampal CA1 area of adult and aged rats,” *Anat. Cell Biol.*, vol. 47, no. 2, p. 117, Jun. 2014.
- [49] C. Ullrich, M. Pirchl, and C. Humpel, “Hypercholesterolemia in rats impairs the cholinergic system and leads to memory deficits,” *Mol. Cell. Neurosci.*, vol. 45, no. 4, pp. 408–417, Dec. 2010.
- [50] P. K. Elias, M. F. Elias, R. B. D’Agostino, L. M. Sullivan, and P. A. Wolf, “Serum Cholesterol and Cognitive Performance in the Framingham Heart Study,” *Psychosom. Med.*, vol. 67, no. 1, pp. 24–30, Jan. 2005.
- [51] L.-J. Li, J.-C. Zheng, R. Kang, and J.-Q. Yan, “Targeting Trim69 alleviates high fat diet (HFD)-induced hippocampal injury in mice by inhibiting apoptosis and inflammation through ASK1 inactivation,” *Biochem. Biophys. Res. Commun.*, vol. 515, no. 4, pp. 658–664, Aug. 2019.

- [52] S. Dutheil, K. T. Ota, E. S. Wohleb, K. Rasmussen, and R. S. Duman, “High-Fat Diet Induced Anxiety and Anhedonia: Impact on Brain Homeostasis and Inflammation,” *Neuropsychopharmacology*, vol. 41, no. 7, pp. 1874–87, 2016.
- [53] S. Hao, A. Dey, X. Yu, and A. M. Stranahan, “Dietary obesity reversibly induces synaptic stripping by microglia and impairs hippocampal plasticity,” *Brain. Behav. Immun.*, vol. 51, pp. 230–239, Jan. 2016.
- [54] S. E. Kanoski, Y. Zhang, W. Zheng, and T. L. Davidson, “The Effects of a High-Energy Diet on Hippocampal Function and Blood-Brain Barrier Integrity in the Rat,” *J. Alzheimer’s Dis.*, vol. 21, no. 1, pp. 207–219, Jul. 2010.
- [55] J. Altman, “Are New Neurons Formed in the Brains of Adult Mammals?,” *Science*, vol. 135, no. 3509, pp. 1127–1128, Mar. 1962.
- [56] E. Gould, “How widespread is adult neurogenesis in mammals?” *Nat. Rev. Neurosci.*, vol. 8, no. 6, pp. 481–488, Jun. 2007.
- [57] M. Schouten, M. R. Buijink, P. J. Lucassen, and C. P. Fitzsimons, “New Neurons in Aging Brains: Molecular Control by Small Non-Coding RNAs,” *Front. Neurosci.*, vol. 6, p. 25, 2012.
- [58] Y. Murata *et al.*, “A high fat diet-induced decrease in hippocampal newly-born neurons of male mice is exacerbated by mild psychological stress using a Communication Box,” *J. Affect. Disord.*, vol. 209, pp. 209–216, Feb. 2017.
- [59] H. R. Park, M. Park, J. Choi, K.-Y. Park, H. Y. Chung, and J. Lee, “A high-fat diet impairs neurogenesis: Involvement of lipid peroxidation and brain-derived neurotrophic factor,” *Neurosci. Lett.*, vol. 482, no. 3, pp. 235–239, Oct. 2010.
- [60] D. N. Hebert and M. Molinari, “In and Out of the ER: Protein Folding, Quality Control, Degradation, and Related Human Diseases,” *Physiol. Rev.*, vol. 87, no. 4, pp. 1377–1408, Oct. 2007.

- [61] D. Ron, "Translational control in the endoplasmic reticulum stress response," *J. Clin. Invest.*, vol. 110, no. 10, pp. 1383–8, Nov. 2002.
- [62] V. M. Parmar and M. Schröder, "Sensing Endoplasmic Reticulum Stress," in *Advances in experimental medicine and biology*, vol. 738, 2012, pp. 153–168.
- [63] P. Walter and D. Ron, "The Unfolded Protein Response: From Stress Pathway to Homeostatic Regulation," *Science (80)*, vol. 334, no. 6059, pp. 1081–1086, Nov. 2011.
- [64] H. P. Harding, Y. Zhang, A. Bertolotti, H. Zeng, and D. Ron, "Perk is essential for translational regulation and cell survival during the unfolded protein response," *Mol. Cell*, vol. 5, no. 5, pp. 897–904, May 2000.
- [65] W. Cui, J. Li, D. Ron, and B. Sha, "The structure of the PERK kinase domain suggests the mechanism for its activation," *Acta Crystallogr. Sect. D Biol. Crystallogr.*, vol. 67, no. 5, pp. 423–428, May 2011.
- [66] H. P. Harding, Y. Zhang, and D. Ron, "Protein translation and folding are coupled by an endoplasmic-reticulum-resident kinase," *Nature*, vol. 397, no. 6716, pp. 271–274, Jan. 1999.
- [67] G. D. Pavitt, "eIF2B, a mediator of general and gene-specific translational control," *Biochem. Soc. Trans.*, vol. 33, no. 6, p. 1487, Dec. 2005.
- [68] E. Kim *et al.*, "eIF2A, an initiator tRNA carrier refractory to eIF2 α kinases, functions synergistically with eIF5B," *Cell. Mol. Life Sci.*, vol. 75, no. 23, pp. 4287–4300, Dec. 2018.
- [69] A. Andaya, N. Villa, W. Jia, C. S. Fraser, and J. A. Leary, "Phosphorylation stoichiometries of human eukaryotic initiation factors," *Int. J. Mol. Sci.*, vol. 15, no. 7, pp. 11523–38, Jun. 2014.

- [70] S. R. Kimball, "Eukaryotic initiation factor eIF2," *Int. J. Biochem. Cell Biol.*, vol. 31, no. 1, pp. 25–9, Jan. 1999.
- [71] K. M. Vattem and R. C. Wek, "Reinitiation involving upstream ORFs regulates ATF4 mRNA translation in mammalian cells," *Proc. Natl. Acad. Sci.*, vol. 101, no. 31, pp. 11269–11274, Aug. 2004.
- [72] I. Novoa, H. Zeng, H. P. Harding, and D. Ron, "Feedback inhibition of the unfolded protein response by GADD34-mediated dephosphorylation of eIF2 α ," *J. Cell Biol.*, vol. 153, no. 5, pp. 1011–22, May 2001.
- [73] H. Nishitoh, "CHOP is a multifunctional transcription factor in the ER stress response," *J. Biochem.*, vol. 151, no. 3, pp. 217–219, Mar. 2012.
- [74] J. Lu *et al.*, "Chronic administration of troxerutin protects mouse brain against d-galactose-induced impairment of cholinergic system," *Neurobiol. Learn. Mem.*, vol. 93, no. 2, pp. 157–164, Feb. 2010.
- [75] W. Scheper and J. J. M. Hoozemans, "The unfolded protein response in neurodegenerative diseases: a neuropathological perspective," *Acta Neuropathol.*, vol. 130, no. 3, pp. 315–331, Sep. 2015.
- [76] T. Ma and E. Klann, "PERK: a novel therapeutic target for neurodegenerative diseases?" *Alzheimers. Res. Ther.*, vol. 6, no. 3, p. 30, 2014.
- [77] J. M. Axten *et al.*, "Discovery of GSK2656157: An Optimized PERK Inhibitor Selected for Preclinical Development," *ACS Med. Chem. Lett.*, vol. 4, no. 10, pp. 964–968, Oct. 2013.
- [78] G. Mercado *et al.*, "Targeting PERK signaling with the small molecule GSK2606414 prevents neurodegeneration in a model of Parkinson's disease," *Neurobiol. Dis.*, vol. 112, pp. 136–148, Apr. 2018.

- [79] J. A. Moreno *et al.*, “Oral Treatment Targeting the Unfolded Protein Response Prevents Neurodegeneration and Clinical Disease in Prion-Infected Mice,” *Sci. Transl. Med.*, vol. 5, no. 206, pp. 206ra138-206ra138, Oct. 2013.
- [80] Y. L. Wong, L. LeBon, R. Edalji, H. Ben Lim, C. Sun, and C. Sidrauski, “The small molecule ISRIB rescues the stability and activity of Vanishing White Matter Disease eIF2B mutant complexes,” *Elife*, vol. 7, Feb. 2018.
- [81] M. Halliday *et al.*, “Partial restoration of protein synthesis rates by the small molecule ISRIB prevents neurodegeneration without pancreatic toxicity,” *Cell Death Dis.*, vol. 6, no. 3, pp. e1672–e1672, Mar. 2015.
- [82] S. Crunkhorn, “Phosphatase inhibitor prevents protein-misfolding diseases,” *Nat. Rev. Drug Discov.*, vol. 14, no. 6, pp. 386–386, Jun. 2015.
- [83] M. A. Brostrom, X. J. Lin, C. Cade, D. Gmitter, and C. O. Brostrom, “Loss of a calcium requirement for protein synthesis in pituitary cells following thermal or chemical stress,” *J. Biol. Chem.*, vol. 264, no. 3, pp. 1638–43, Jan. 1989.
- [84] I. Novoa, Y. Zhang, H. Zeng, R. Jungreis, H. P. Harding, and D. Ron, “Stress-induced gene expression requires programmed recovery from translational repression,” *EMBO J.*, vol. 22, no. 5, pp. 1180–1187, Mar. 2003.
- [85] I. Das *et al.*, “Preventing proteostasis diseases by selective inhibition of a phosphatase regulatory subunit,” *Science (80)*, vol. 348, no. 6231, pp. 239–242, Apr. 2015.
- [86] C. Kursungoz, M. Ak, and T. Yanik, “Effects of risperidone treatment on the expression of hypothalamic neuropeptide in appetite regulation in Wistar rats,” *Brain Res.*, vol. 1596, pp. 146–155, Jan. 2015.
- [87] M. M. Adams *et al.*, “Caloric restriction and age affect synaptic proteins in hippocampal CA3 and spatial learning ability,” *Exp. Neurol.*, vol. 211, no. 1, pp. 141–149, May 2008.

- [88] B. Aşkın, “Assessment of the impacts of hyperlipidemia on brain and modulation of PERK pathway against hyperlipidemia-induced synaptic impairment on hippocampus,” M.S. Thesis, METU, Ankara, Turkey, 2019.
- [89] C. A. Dinarello, “Interleukin-1, Interleukin-1 Receptors and Interleukin-1 Receptor Antagonist,” *Int. Rev. Immunol.*, vol. 16, no. 5–6, pp. 457–499, Jan. 1998.
- [90] J. Spampanato, R. K. Sullivan, F. R. Turpin, P. F. Bartlett, and P. Sah, “Properties of doublecortin expressing neurons in the adult mouse dentate gyrus.,” *PLoS One*, vol. 7, no. 9, p. e41029, 2012.
- [91] V. V. Guselnikova and D. E. Korzhevskiy, “NeuN As a Neuronal Nuclear Antigen and Neuron Differentiation Marker.,” *Acta Naturae*, vol. 7, no. 2, pp. 42–7, 2015.
- [92] S. E. Kanoski and T. L. Davidson, “Western diet consumption and cognitive impairment: Links to hippocampal dysfunction and obesity,” *Physiol. Behav.*, vol. 103, no. 1, pp. 59–68, Apr. 2011.
- [93] N. Castanon, G. Luheshi, and S. Layé, “Role of neuroinflammation in the emotional and cognitive alterations displayed by animal models of obesity,” *Front. Neurosci.*, vol. 9, p. 229, Jul. 2015.
- [94] K. Pakos-Zebrucka, I. Koryga, K. Mnich, M. Ljujic, A. Samali, and A. M. Gorman, “The integrated stress response,” *EMBO Rep.*, vol. 17, no. 10, pp. 1374–1395, Oct. 2016.
- [95] C. Ma, Z. Yin, P. Zhu, J. Luo, X. Shi, and X. Gao, “Blood cholesterol in late-life and cognitive decline: a longitudinal study of the Chinese elderly,” *Mol. Neurodegener.*, vol. 12, no. 1, p. 24, Dec. 2017.
- [96] J. G. Fox, S. Barthold, M. Davisson, C. E. Newcomer, and F. W. Quimby, *The Mouse in Biomedical Research, Volume 4: Immunology*. Elsevier, 2006.

- [97] S. E. Arnold *et al.*, “High fat diet produces brain insulin resistance, synaptodendritic abnormalities and altered behavior in mice,” *Neurobiol. Dis.*, vol. 67, pp. 79–87, Jul. 2014.
- [98] G. Lo Sasso, W. K. Schlage, S. Boué, E. Veljkovic, M. C. Peitsch, and J. Hoeng, “The Apoe(-/-) mouse model: a suitable model to study cardiovascular and respiratory diseases in the context of cigarette smoke exposure and harm reduction,” *J. Transl. Med.*, vol. 14, no. 1, p. 146, 2016.
- [99] C. I. F. Janssen *et al.*, “The Effect of a High-Fat Diet on Brain Plasticity, Inflammation and Cognition in Female ApoE4-Knockin and ApoE-Knockout Mice,” *PLoS One*, vol. 11, no. 5, p. e0155307, May 2016.
- [100] N. Pilati, M. Barker, S. Panteleimonitis, R. Donga, and M. Hamann, “A Rapid Method Combining Golgi and Nissl Staining to Study Neuronal Morphology and Cytoarchitecture,” *J. Histochem. Cytochem.*, vol. 56, no. 6, pp. 539–550, Jun. 2008.
- [101] A. Kádár, G. Wittmann, Z. Liposits, and C. Fekete, “Improved method for combination of immunocytochemistry and Nissl staining,” *J. Neurosci. Methods*, vol. 184, no. 1, pp. 115–8, Oct. 2009.

APPENDIX A

A. Supplementary for Western Blot Analysis

Table A.1. The preparation of blank and standards.

	ddH ₂ O (ul)	BSA(ul) (from 1mg/1mL stock solution)	Concentration values (ug/mL)
Blank	5	0	0
Standard 1	4,5	0,5	2
Standard 2	4	1	4
Standard 3	3	2	8
Standard 4	2	3	12
Standard 5	1	4	16
Standard 6	0	5	20

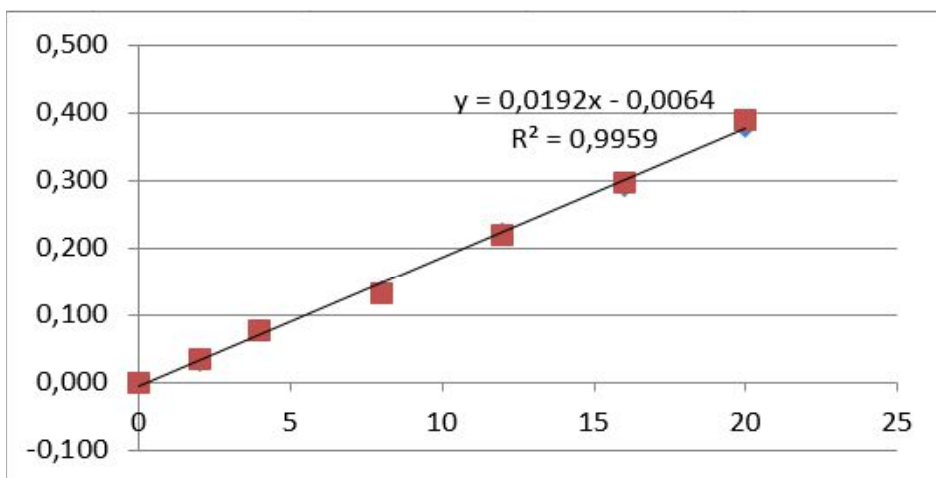


Figure A.1. The standard curve of the absorbance levels of standards.

Table A.2. 10mL of 12% running gel.

Components	Amounts
Water	3.0 mL
40 % Acrylamide/bis	3.0 mL
1 M Tris-HCl, pH 8.8	3.750 mL
10 % SDS	100 μ l
10 % APS	100 μ l
TEMED	10 μ l

Table A.3. 5mL of 5% stacking gel.

Components	Amounts
Water	3.770 mL
40 % Acrylamide/bis	0.500 mL
1 M Tris-HCl, pH 8.8	0.625 mL
10 % SDS	50 μ l
10 % APS	50 μ l
TEMED	5 μ l

Table A.4. 10X SDS-PAGE Running buffer.

Components	Amounts
Tris Base (25mM)	30 g
Glycine (192 mM)	144 g
Sodium Dodecyl Sulfate	10 g
Water	1000 mL

Table A.5. 10X Transfer Buffer.

Components	Amounts
Tris Base	30 g
Glycine	144 g
Water	1000 mL

Table A.6. 10X TBS adjusted at pH:7.6.

Components	Amounts
Tris Base	24.2 g
NaCl	80.0 g
dH ₂ O	1 liter